Permanent WRAP URL:
http://wrap.warwick.ac.uk/89166

A note on versions:
The version presented here may differ from the published version or, version of record, if you wish to cite this item you are advised to consult the publisher's version. Please see the 'permanent WRAP url' above for details on accessing the published version and note that access may require a subscription.

For more information, please contact the WRAP Team at: wrap@warwick.ac.uk

warwick.ac.uk/lib-publications

Optimal management of nutrient reserves in microorganisms under time-varying environmental conditions

Olga A. Nev[a,1], Oleg A. Nev[b], Hugo A. van den Berg[a,*]

[a]*Warwick Analytical Sciences Centre, University of Warwick, Coventry, CV4 7AL UK*
[b]*Independent software developer, Nizhny Novgorod, Russia*

Abstract

Intracellular reserves are a conspicuous feature of many bacteria; such internal stores are often present in the form of inclusions in which polymeric storage compounds are accumulated. Such reserves tend to increase in times of plenty and be used up in times of scarcity. Mathematical models that describe the dynamical nature of reserve build-up and use are known as "cell quota," "dynamic energy/nutrient budget," or "variable-internal-stores" models. Here we present a stoichiometrically consistent macro-chemical model that accounts for variable stores as well as adaptive allocation of building blocks to various types of catalytic machinery. The model posits feedback loops linking expression of assimilatory machinery to reserve density. The precise form of the "regulatory law" at the heart of such a loop expresses how the cell manages internal stores. We demonstrate how this "regulatory law" can be recovered from experimental data using several empirical data sets. We find that stores should be expected to be negiglibly small in stable growth-sustaining environments, but prominent in environments characterised by marked fluctuations on time scales commensurate with the inherent dynamic time scale of the organismal system.

Keywords: microbial growth, nutrient limitation, cell quota, cellular resource allocation, optimal regulation, fitness, evolutionary adaptation

1. Introduction

Many bacteria form intracellular reserves, in particular during so-called "feast" periods of growth: when nutrients are available from the ambient environment at relatively high levels, bacterial cells accumulate polymers that can be degraded to fuel metabolism during subsequent periods of "famine" when nutrients are absent from the environment or present at such low levels that they do not suffice to meet the cell's maintenance requirements (Preiss, 1989). In prokaryotes reserves occur as metabolite pools, reserve compounds, granules, and elemental inclusions (Beveridge, 1989; Preiss, 1989; Neidhardt et al., 1990). Whether the organism can continue to meet

---

the requirements of endogenous metabolism for the entire duration of the "famine" depends on the amount of accumulated reserves. For instance, in experiments involving *Escherichia coli* growing on carbon as a limiting factor (Holme and Palmstierna, 1956), the level of the carbon reserve compound glycogen accumulated by the cell was about 6–7% of the dry weight, which supported a cell during a starvation period of 15 hours. Similar results were obtained with *Rodospirillum ruborem* growing on acetate or butyrate and accumulating poly-β-hydroxybutyrate (Doudoroff and Stanier, 1959).

The accumulation of reserves can be viewed as an adaptation to fluctuating environmental conditions, which prompts us to ask at what rate the cell should allot core metabolites to the formation of reserves during the "feast" periods. This question can be framed as an evolutionary one: what kind of reserve management strategy maximises fitness? Any attempt at an answer must presuppose that there is a sensible way to quantify fitness in the context of microbial ecology. The specific growth rate μ, defined as the rate of change of the natural logarithm of the biomass, has long been viewed as a natural measure of fitness (Lenski et al., 1991). However, this is not valid in general (van den Berg, 2015); in particular, the growth rate is generally a function of time t and it can be shown that the manner in which the function $\mu(t)$ should be "discounted" over the long-term time integral strongly depends on ecological circumstances; for instance, if we consider an ecotype in which the need to outcompete competitors (in the short term, whenever the latter arrive) is paramount, we find that we should derive a different fitness measure as compared to an ecotype in which competition is not a dominant effect, but in which the cells form spores whenever they enter a spell of nutrient shortage (van den Berg et al., 2008). Here, we consider an ecological setting in which one can assume as valid the definition proposed by Metz and co-workers (Metz et al., 1992, 1995), namely that fitness is the eventual asymptotic growth rate of a colony that remains sufficiently small so as not to affect the state of the environment. To isolate the problem of interest, selective pressure is taken to derive solely from fluctuations in environmental availability of a nutrient; in particular, we assume that there are no competing types and the bacterial cell does not sporulate but has to survive periods of famine as a viable cell that has the ability to reduce endogenous metabolism under conditions of severe starvation.

To address the question of optimal (maximally adaptive) regulation of reserve accumulation and mobilisation we require, in addition to a quantitive measure of fitness, a suitable parametrisation of the regulatory phenotype. The biochemical and genetic particulars are intricate and highly variable between different species (Dawes, 1989), suggesting that optimisation would be challenging in view of the high-dimensional parameter spaces of mathematical models at this level of detail. One solution is to tackle the problem at the higher, aggregated level of macro-chemical kinetics models, also known as "variable-internal-stores" models (Williams, 1967; Droop, 1968; Grover, 1991). We previously proposed that the regulation of internal stores in such models can be represented by so-called "regulatory" functions that link the physiological state of the cell (in the case at hand: the reserve levels) to the allocation of molecular building blocks to various types of catalytic machinery (Nev and van den Berg, 2017b). At the biochemically detailed level, this allocation is mediated by regulation of transcription (Kramer et al., 2010): *ceteris paribus*, more of a given enzyme will be synthesised if the level of mRNA encoding that enzyme is increased (although numerous additional factors impinge on this causal connection; Neidhardt et al., 1990).

The aims of the present paper are, first, to support the notion of such regulatory functions, which we will call "*r*-functions" in what follows, by demonstrating how they can be explicitly reconstructed from experimental data; and second, to study the simplest example of an *r*-function, specifically a decreasing sigmoid, and determine the optimal-fitness combination of the shape parameters of this function faced with an environment that switches between "feast" and "famine" in a predictable and regular fashion, and to understand the evolutionary optima we obtain in terms of the physiological dynamics of the cell.

The paper is organised as follows. In Section 2 we briefly review the theory of macro-chemical kinetics with variable internal stores, as presented in our previous papers (Nev and van den Berg, 2017a,b). In Section 3 we describe and demonstrate the reconstruction of regulatory rules, represented as *r*-functions, from observational data. The notion of *r*-functions was introduced in our earlier work but is here confronted with experimental data. Finally, in Section 4, we address the problem of evolutionarily optimal regulation of reserve density, which was not considered in the earlier papers.

2. Macro-chemical kinetics

Before describing the reconstruction of regulatory rules, implemented here as "*r*-functions," we recapitulate the basic model so as to render the present paper reasonably self-contained (this section overlaps with our previous work).

The model (Nev and van den Berg, 2017a,b) distinguishes $n+2$ types of molecular machinery, where n corresponds to the number of different chemical species of nutrients in the environment. In addition to *synthetic* machinery (RNA transcriptase, ribosomes, and the associated molecular components) and *growth* machinery (DNA replicase and machinery involved in cell envelope synthesis) there is a dedicated type of machinery for the *uptake* of each of the n nutrients. The C-molar amounts of these $n+2$ types of machinery are denoted as M_i for $i \in \{0, 1, \ldots, n, G\}$, where the index 0 stands for synthetic machinery, G for growth machinery, and 1 through n for assimilatory machineries. *Reserve* components are likewise expressed in C-moles, or, if carbon is not part of their chemical composition, in terms of the molar amount of their dominant element X_j. These amounts are denoted as X_j for $j \in \{1, \ldots, n\}$.

The *structural* component, finally, includes the cell envelope, as well as the genetic material and the small molecules of metabolism, the intermediates of catabolic and anabolic pathways which are maintained at appropriate cellular concentrations. The C-molar amount of the structural component is denoted by W. Table 1 characterises the components in terms of the major classes of proteins that are assigned to them.

The dynamics of each component is given by the following expression:

$$\dot{M}_i = \alpha_i M_0 \widetilde{\phi}_i, \quad i \in \{0, 1, \ldots, n, G\}, \tag{1}$$

where α_i is the allocation coefficient describing which portion of (the time of) the basic catalytic machinery M_0 is dedicated to the synthesis of the ith component, and $\widetilde{\phi}_i$ is a stoichiometric coefficient (a tilde is used to mark parameters prior to scaling). The allocation coefficients α_i are all non-negative and satisfy $\sum_{i \in \{0,1,\ldots,n,G\}} \alpha_i = 1$. In principle, these coefficients should be

Table 1: Assignment of major classes of proteins, grouped according to function, to macro-chemical components in a typical *E. coli* cell

ine Synthetic M_0	Uptake $M_1,\ldots,M_n$	Growth M_G	Structural W
ine Ribosome-related	Nutrient uptake	Agmatine synthesis	Catabolism
Ribosomal	Core metabolism	Amino-acid synthesis	Chaperones/folding
RNA-related		Cell division	Chemotaxis
Transcriptional		Cell envelope synthesis	Defense
Translational		Cofactor synthesis	Metabolic intermediates
		DNA replication	Repair
		Fatty acid synthesis	RNA degradation
		Glutamate synthesis	RNA modification
		Glutamine synthesis	Secretion
		Glutathione synthesis	Storage-related
		Protein synthesis	Transcriptional repressors
		Protoporphyrin synthesis	Cell envelope
		Selenophosphate synthesis	Redox reactions
		Spermidine synthesis	
		Sulfide synthesis	

See Table A.2 in Appendix A for a detailed account assigning all known individual proteins.

treated as time-varying; they depend on the "regulatory state" of the organism. A particularly simple feedback model for the α_i is used in the present study, eqn (7) below.

Growth (or more precisely, structural growth) is the rate of change of W and is proportional to M_G, as follows:

$$\dot{W} = \widetilde{\psi}_W M_G .\tag{2}$$

Summing over all gain and loss terms we obtain the dynamics of reserve component j:

$$\dot{X}_j = \sum_{i=1}^{n} \widetilde{\psi}_{ji} M_i - \widetilde{\sigma}_{jW}\dot{W} - M_0 \sum_{i\in\{0,1,\ldots,n,G\}} \widetilde{\sigma}_{ji}\alpha_i\widetilde{\phi}_i - \widetilde{c}_j W , \quad i \in \{0,1,\ldots,n,G\} , j \in \{1,\ldots,n\} .\tag{3}$$

Here the first term represents gains due to uptake; the second term represents expenditure on structural growth (increase of W); the third term represents investment in catalytic machinery; and the final term represents "maintenance," dissimilatory expenditure on endogenous metabolism (Herbert, 1958; Marr et al., 1962; Pirt, 1965). Thus, $\widetilde{\psi}_{ji}$ is the gain of reserve j per unit machinery of type i; $\widetilde{\sigma}_{jW}$ is the loss of reserve j per unit increase of W; $\widetilde{\sigma}_{ji}$ is the loss of reserve j per unit synthesis of machinery of type i; $\widetilde{c}_j$ is the maintenance cost of reserve j that is being catabolised per unit of W. The specific growth rate $\widetilde{\mu}$ equals $\frac{d}{dt}\ln W(t)$ by definition.

Choosing $\widetilde{\phi}_0^{-1}$ as a unit of time, we render the equations dimensionless, by defining the following scaled variables:

$$m_i = \frac{M_i\widetilde{\phi}_0}{W\widehat{m}\widetilde{\phi}_i} ; \qquad x_j = \frac{X_j}{W\widetilde{\sigma}_{jW}} ,\tag{4}$$

where $\widehat{m}$ is chosen such that $m_0 \equiv M_0/W$ is maintained at the dimensionless value 1 via the r-function for growth (Nev and van den Berg, 2017b). Scaled stoichiometric parameters are defined as follows:

$$\psi_{ji} = \frac{\widetilde{\psi}_{ji}\,\widetilde{\phi}_i\,\widehat{m}}{\widetilde{\sigma}_{jW}\,\widetilde{\phi}_0^2}\;;\qquad \psi_W = \frac{\widetilde{\psi}_W\,\widetilde{\phi}_G\,\widehat{m}}{\widetilde{\phi}_0^2}\;;\qquad \sigma_{ji} = \frac{\widetilde{\sigma}_{ji}\,\widetilde{\phi}_i\,\widehat{m}}{\widetilde{\sigma}_{jW}\,\widetilde{\phi}_0}\;;\qquad c_j = \frac{\widetilde{c}_j}{\widetilde{\sigma}_{jW}\,\widetilde{\phi}_0}\;. \tag{5}$$

We assume $\sigma_{ji} = \sigma_j$ for every reserve j, which is reasonable as different types i of machinery can be taken to be biochemically similar. Also, for the sake of simplicity we assume $\psi_{ji} = 0$ whenever $j \neq i$ and write $\psi_{jj} \equiv \psi_j$. The scaled system of differential equations is as follows:

$$\begin{cases} \dot{x}_j = \psi_j m_j - \mu\left(1+x_j\right) - m_0\sigma_j - c_j & \text{for } j \in \{1,\ldots,n\} \\ \dot{m}_i = \alpha_i m_0 - \mu m_i & \text{for } i \in \{0,1,\ldots,n,G\}\,. \end{cases} \tag{6}$$

The link between reserve densities and synthesis of catalytic machinery is encoded by allocation coefficients α_j which are given by the following expressions:

$$\alpha_0 = (1+r_1+\cdots+r_n+r_G)^{-1}\;;\quad \alpha_j = r_j\alpha_0 \quad \text{for } 1 \le j \le n\,,\quad j = G\,, \tag{7}$$

where $r_1,\ldots,r_n,r_G$ are the r-functions. These are functions that are in general assumed to depend on the (intensive) state of the cell (i.e. the variables $\{m_0,m_1,\ldots,m_n,m_G,x_1,\ldots,x_n\}$, perhaps augmented with whatever additional state variables are required to describe the regulatory behaviour of the organism). In the present (simplest) incarnation of the model, r_j is assumed to be a decreasing sigmoid function of the reserve density x_j for $1 \le j \le n$ and r_G is assumed to be a steeply increasing sigmoid function of m_0, with a midpoint at $m_0 = 1$. The latter is consistent with observations on the relationship between the cell's RNA content and the specific growth rate (Herbert, 1961).

Under constant and growth-sufficient environmental conditions (i.e., the coefficients ψ_j are constant in time and permit growth at a strictly positive rate), the system (6) has a unique and stable equilibrium point (Nev and van den Berg, 2017b), characterised by the following equations:

$$\mu = \alpha_0 = \left(1+\sum_{i\in\{1,\ldots,n,G\}} r_i\right)^{-1}, \tag{8}$$

$$m_i = r_i m_0 \quad \text{for } i \in \{1,\ldots,n,G\}\,, \tag{9}$$

$$\psi_j r_j = \psi_W r_G(1+x_j) + \sigma_j + c_j/m_0 \quad \text{for } j \in \{1,\ldots,n\}\,, \tag{10}$$

where $\mu = (W\widetilde{\phi}_0)^{-1}\dot{W} = \psi_W m_G$ is the specific growth rate expressed in scaled time.

Numerical estimates for the scaled parameters can be obtained by considering the stoichiometry of a typical prokaryotic cell, as described in detail in Appendix A. We usually focus on *intensive* scaled state variables $\{m_0,m_1,\ldots,m_n,m_G,x_1,\ldots,x_n\}$, which represent densities, rather than the corresponding *extensive* variables $\{M_0,M_1,\ldots,M_n,M_G,X_1,\ldots,X_n\}$, which are proportional to the structural biomass W; it is the intensive variables that can plausibly be assumed to be represented by intracellular signals.

3. Data-driven reconstruction of the r-function

In the context of macro-chemical kinetics models such as described in the foregoing section, r-functions serve as linker functions that connect the physiological state of the cell to the relative rates of synthesis of new catalytic machinery (Nev and van den Berg, 2017b). We here focus on what is perhaps the most elementary specification for the r-function, namely one that links reserve density to the allocation of molecular building blocks to the machinery devoted to the uptake of the nutrient that is stored.

The equilibrium conditions lead to the following pair of equations for $n = 1$:

$$x_1 = \psi_1 \left(\mu^{-2} - \mu^{-1} - \psi_W^{-1} \right) - \left(1 + \sigma_1/\mu + c_1/\mu \right) \tag{11}$$

$$r_1 = \mu^{-1} - 1 - \mu/\psi_W \tag{12}$$

(Nev and van den Berg, 2017b). Thus, given a set of observations performed at various values of $\widetilde{\mu}$ under steady-state conditions, we can calculate x_1 and r_1 and plot them as pairs (x_1, r_1), obtaining a scatter plot that gives a graphical representation of the regulatory law $r_1(x_1)$. For the purposes of subsequent analysis, it is usually convenient to fit a suitable empirical function to these data; we shall employ the following sigmoid function:

$$r_1 = \zeta_1 + \widehat{r}_1 \left(1 + \exp\{\vartheta_1 \left(x_1 - \xi_1 \right)\} \right)^{-1}, \tag{13}$$

which has two shape parameters, a midpoint location parameter ξ_1 and a midpoint slope parameter ϑ_1, as well as a scaling parameter $\widehat{r}_1$ and an offset parameter ζ_1.

As eqns (11) and (12) make clear, the essential challenge is to estimate the scaled reserve density x_1 from the data, inasmuch as r_1 is readily deduced from the scaled specific growth rate μ (along with the scaled parameter ψ_W, which is estimated in Appendix A). Different strategies must be adopted, depending on the type of data available. For instance, Schulze and Lipe (1964) provide data on the yield of *E. coli* grown on glucose, defined as the amount of biomass Y gained per unit of glucose taken up by the cell mass (Fig. 1, left panel). If we assume that the yield at $\widetilde{\mu} = 0$ corresponds to lean cells devoid of glycogen surplus, we can regard the difference between $Y(\widetilde{\mu})$ and $Y_0 = Y(\widetilde{\mu})|_{\widetilde{\mu}=0}$ as a measure for the glycogen surplus present at $\widetilde{\mu}$. Taking 0.45 as the weight fraction occupied by structural biomass W within this lean cell composition (see Appendix A), we are able to estimate the structural weight corresponding to $Y - Y_0$ as $0.45Y_0$. The scaled reserve density x_1 can then be calculated using eqn (4) where the numerical value of $\widetilde{\sigma}_{1,W}$ is provided by the calculations outlined in Appendix A. The transformed data (x_1, r_1) together with the best-fitting empirical form, eqn (13), are shown in Fig. 1, right panel.

Direct observations on the reserve density are available in some cases. For instance, Rhee (1973) estimated phosphate reserves in the green alga *Scenedesmus sp.*, grown under phosphorus-limited conditions, by means of two different analytical methods ("surplus P" and "total polyphosphates"). The scaled reserve density x_1 can then be directly calculated, using the estimate for the mass of structural biomass per cell (Appendix A). The results are shown in Fig. 2.

More generally, however, the available chemical-analytical methods do not permit a specific assignment of the particle species of interest to reserve versus non-reserve biomass, or do so only imperfectly. In these instances, the *cell quota* concept introduced by Droop (1968) is useful: one
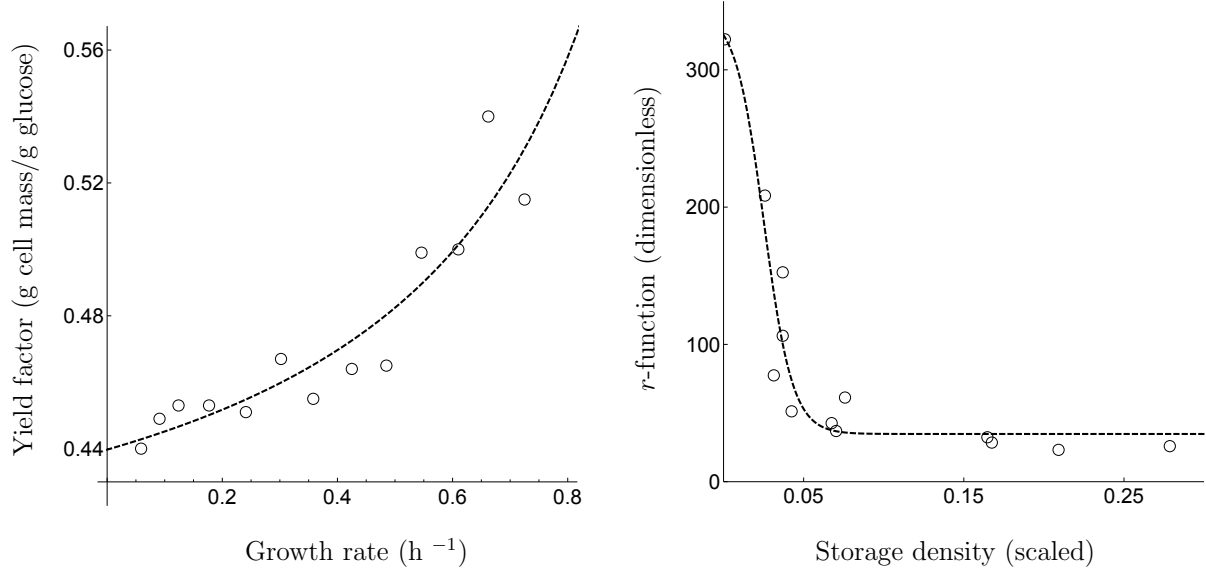
Figure 1: Reconstruction of the *r*-function for *Escherichia coli* grown under carbon-limited conditions (the limiting nutrient is glucose). Left: original data taken from Schulze and Lipe (1964), together the optimal non-linear least-squares fit of eqn $y = c + a/(b-x)$ with parameters $a = 0.074$; $b = 1.2$; $c = 0.38$. Right: transformed data, together with the optimal non-linear least-squares fit of eqn (13) with parameters $\widehat{r}_1 = 307.84$; $\vartheta_1 = 111.65$; $\xi_1 = 0.025$; $\zeta_1 = 34.76$.

simply states the total over all components and reports this figure on a per-cell basis. Calculating x_1 and r_1 on the basis of cell quota data is more involved but it has the advantage that it is applicable for general $n \geq 1$.

Let $\widetilde{\widetilde{\phi}}_j f_j M_j$ denote the flux of the corresponding nutrient through the assimilatory machinery of type j, where $\widetilde{\widetilde{\phi}}_j$ corresponds to a maximum rate per unit of machinery (e.g. when the latter is fully saturated by excess of substrate in the environment) and $f_j \in [0,1]$ expresses ambient conditions (e.g. eqn (15) below). In view of the scaling for M_j, eqn (4) and the equilibrium conditions, eqns (8)–(10), we have the following expression for the nutrient uptake flux via machinery of type j:

$$\widetilde{\widetilde{\phi}}_j f_j \frac{\widetilde{\phi}_j}{\widetilde{\phi}_0} r_j W \widehat{m} .$$

At steady state, an alternative and equally valid expression for the flux is available in terms of the cell quota Q_j, a concept introduced by Droop (1968), who expressed the nutrient uptake through assimilatory machinery of type j as $Q_j W \widetilde{\mu}$, where $\widetilde{\mu} = \frac{d}{dt} \ln W(t)$ is the unscaled specific growth rate. Equating these two expressions and solving for the *r*-function we find:

$$r_j = \frac{\widetilde{\phi}_0 \widetilde{\mu} Q_j}{\widetilde{\widetilde{\phi}}_j \widetilde{\phi}_j \widehat{m} f_j} , \qquad (14)$$

which can be viewed as a product of two factors: $\widetilde{\mu} Q_j / f_j$, composed of three quantities that
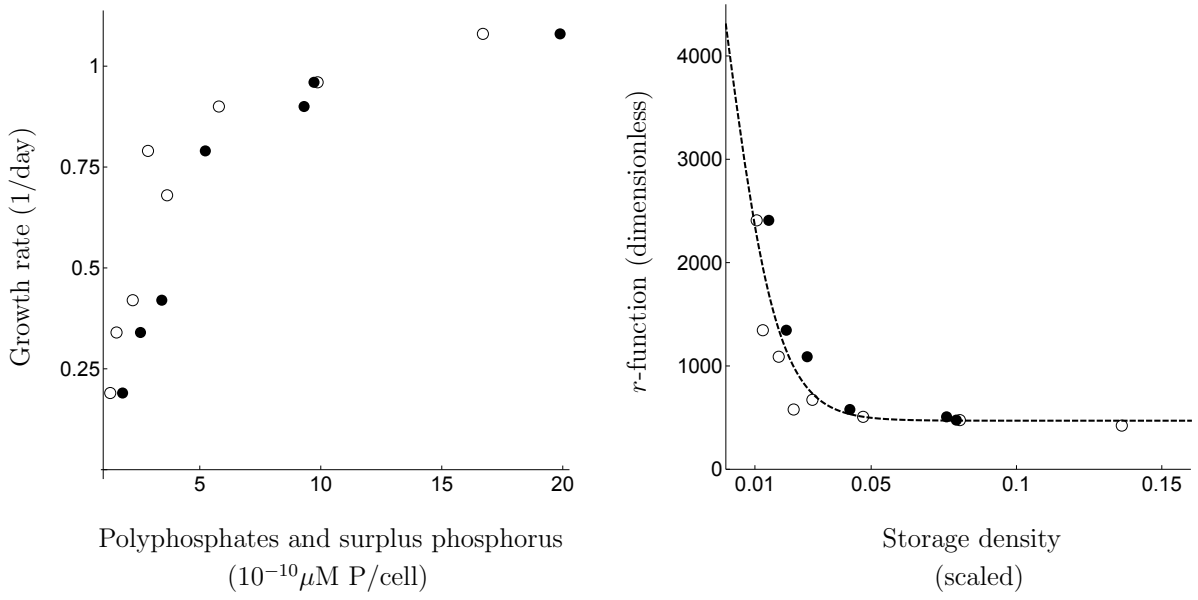
7

Figure 2: Reconstruction of the *r*-function for *Scenedesmus sp.* grown under phosphorus-limited conditions (the limiting nutrient is phosphate). Left: original data taken from Rhee (1973). Right: transformed data, together with the optimal non-linear least-squares fit of eqn (13) with parameters $\widehat{r}_1 = 7668.8$; $\vartheta_1 = 112.1$; $\xi_1 = 2.25 \times 10^{-9}$; $\zeta_1 = 470.3$. Open and filled circles correspond, respectively, to the values of surplus P and total polyphosphates taken from Rhee (1973).

can be estimated from empirical data, and a proportionality constant which is a compound parameter condensing stoichiometric coefficients; numerical estimates of the latter on the basis of independent data are discussed in Appendix A.

An often-employed model that relates f_j to ambient conditions is the Michaelis-Menten hyperbola (van den Berg, 2011):

$$f_j = (1 + K_j/[\mathrm{N}_j])^{-1} \,, \tag{15}$$

where $[\mathrm{N}_j]$ denotes the ambient concentration of the nutrient and K_j is the saturation constant. On this relationship, eqn (14) becomes:

$$r_j = \frac{Q_j \widetilde{\mu} \widetilde{\phi}_0 (1 + K_j/[\mathrm{N}_j])}{\widetilde{\widehat{\phi}}_j \widetilde{\phi}_j \widehat{m}} \,. \tag{16}$$

The cell quota is given by the following equation:

$$Q_j = \kappa_W + \kappa_{m,0} m_0 + + \kappa_{m,G} m_G + \sum_{\ell=1}^{n} \left(\kappa_{m,\ell} m_\ell + \kappa_{x,\ell} x_\ell \right) \,, \tag{17}$$

where $\kappa_\star$ accounts for the amount of nutrient that is incorporated per scaled unit of the corresponding component $\star$; numerical estimates of these coefficients, on the basis of independent data, are discussed in Appendix A. In general, we thus obtain a linear system which can be solved for $x_1, \ldots, x_n$.
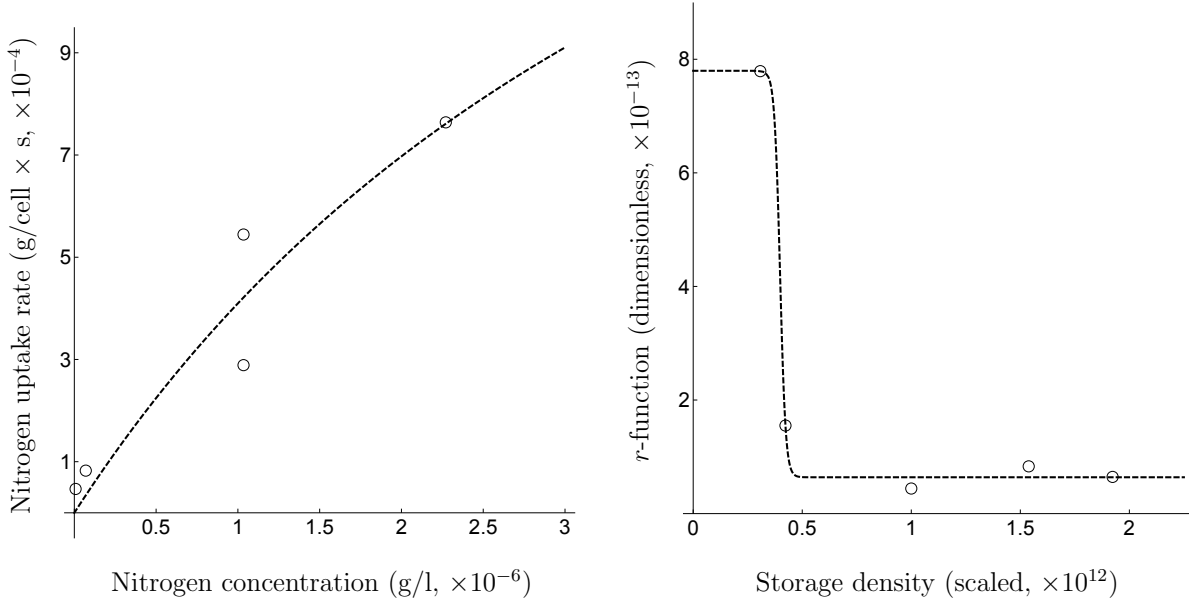
8

Figure 3: Reconstruction of the *r*-function for *Skeletonema costatum* grown under nitrogen-limited conditions (the limiting nutrient is ammonium). Left: original data taken from Harrison et al. (1976), together with the optimal non-linear least-squares fit of eqn (18) with parameters $K_1 = 4.7 \times 10^{-6}$ g/l; $\widetilde{\widetilde{\phi}}_1 = 3.3 \times 10^9$ g per g of uptake machinery per second. Right: transformed data based on cell quota data from Harrison et al. (1976), together with the optimal non-linear least-squares fit of eqn (13) with parameters $\widehat{r}_1 = 7.2 \times 10^{-13}$; $\vartheta_1 = 77.6 \times 10^{-12}$; $\xi_1 = 0.4 \times 10^{12}$; $\zeta_1 = 0.64 \times 10^{-13}$.

In practice, it is convenient to begin by estimating the parameters K_j and $\widetilde{\widetilde{\phi}}_j$ by means of the least-squares criterion, on the basis of the experimental data of the form $\{u_j, [\mathrm{N}_j]\}$, where $u_j = Q_j \widetilde{\mu}$ is the uptake rate of the corresponding nutrient N_j. According to the Michaelis-Menten relationship, eqn (15), u_j depends on N_j as follows:

$$u_j = \widetilde{\widetilde{\phi}}_j (1 + K_j/[\mathrm{N}_j])^{-1} \,. \tag{18}$$

Applying this procedure to data pertaining to the diatom *Skeletonema costatum* grown under nitrogen-limited conditions, we obtain the result shown in Fig. 3.

It can be seen that the sigmoid function, eqn (13), is adequate for the three data sets considered here. The good agreements suggest that the *r*-function, which might be dismissed as a mere conceptual device to provide mathematical closure for the macro-chemical kinetics equations, can be regarded as reified by the data to some extent. It is best thought of as a *grosso modo* description of the regulatory feedback mechanisms in the organism.

A striking difference between the three examples shown is the relative steepness of the sigmoid which corresponds to how stringently the reserve is regulated to the midpoint value ξ_1. Provided that the range of *r*-values allowed by ζ_1 and $\widehat{r}_1$ is great enough, the variation in r_1 is translated into an adapative re-allocation of molecular building blocks toward the corresponding uptake machinery. If the range is great enough and the sigmoid is steep, even small variations

9

will translate into large swings in how building blocks are allocated to the various types of machinery, and thus the growth rate is rapidly adjusted to a value commensurate with maintaining the reserves at level ξ_1 under the prevailing ambient conditions. If the steepness is smaller (and also if the range between ζ_1 and $\widehat{r}_1$ is smaller), the cell allows a certain range of variation of the reserve density, i.e. reserve homeostasis is less stringent.

From a biological point of view, it is almost self-evident that the shape parameters of the r-function, which express how the organism manages its reserves, assume values in response to selective pressure. In other words, the parameter values that characterise a particular organism, for a given type of nutrient reserve, are presumed to constitute an evolutionary optimum. In the remainder of this paper, we explore the hypothesis that this is the case, and investigate in particular the problem of optimality in the face of ambient fluctuations in nutrient availability.

4. Evolutionary adaptation of the r-function

In order to assess evolutionary optimality of the design parameters in any given biological system, a suitable criterion of optimality is required. This is the fitness (or more precisely, the *marginal* fitness) associated with the parameter set $\{\xi_j, \vartheta_j, \widehat{r}_j, \zeta_j\}_{j=1,\ldots,n}$. For microorganisms, the specific growth rate $\widetilde{\mu}(t) \equiv \frac{d}{dt} \ln W(t)$ is an obvious candidate: if two competing types are characterised by the values $\widetilde{\mu}_A$ and $\widetilde{\mu}_B$, the relative abundance of type A with respect to B is expected to grow as $\exp\{\widetilde{\mu}_A - \widetilde{\mu}_B\}$ and thus the condition $\widetilde{\mu}_A > \widetilde{\mu}_B$ amounts to the statement that A is fitter than B. Although this argument seems to have gained currency among microbiologists (e.g., Lenski et al., 1991) it is readily shown by means of elementary counterexamples that instantaneous fitness can be problematic and, in particular, that the ecophysiology of the organism dictates which regime of discounting $\widetilde{\mu}(t)$ over time t is the appropriate measure of fitness (van den Berg et al., 2008).

A suitable definition of fitness in this context is the long-time average specific growth rate, defined as follows:

$$\rho = \lim_{t \to \infty} \frac{\ln W(t)}{t} \tag{19}$$

(cf. Metz et al., 1992). For the practical purposes of estimating fitness via numerical simulations, we use a sufficiently large averaging time to approximate this limit.

4.1. Optimal regulation in a constant environment

Consider the model with $n \geq 1$ types of reserves, subjected to a time-constant environment characterised by the parameters $\{\psi_1, \ldots, \psi_n\}$ with all constants ψ_j strictly positive and growth-sufficient. In such an environment, the optimal r-function for all reserves j is characterised by the double limit $\vartheta_j \to \infty$; $\xi_j \to 0$ $\forall j$. To see this, first observe that this condition is equivalent to $x_j \equiv 0$ $\forall j$, eventually as $t \to \infty$, as a result of the adaptive re-allocation property of the model; in other words we are disregarding any transient behaviour for small t and consider the model in steady state, eqns (8)–(10).

We thus have to establish optimality of the condition $x_j \equiv 0$ $\forall j$, which, in view of the fact that $x_j < 0$ is not permitted in the theory for any j (cf. Nev and van den Berg, 2017a), amounts

10

to showing that any set of non-negative reserve density values $\{x_1, \ldots, x_n\}$ is sub-optimal whenever at least one element is strictly positive. Without loss of generality, relabelling reserves and corresponding nutrient species if necessary, we may assume that x_1 is strictly positive.

Consider the ray emanating from the origin and passing through the point $(x_1, \ldots, x_n)$. The distance between this point and the origin is

$$R = x_1 \sqrt{1 + \eta_2^2 + \cdots + \eta_n^2}, \tag{20}$$

where the parameters $\eta_j = x_j/x_1$, $1 < j \leq n$, are fixed along the ray. We consider the rate of change of the steady-state value of μ as we move along this ray. From eqns (20) and (8)–(10) we find:

$$\frac{d\mu}{dR} = \frac{-\mu \left(\psi_1^{-1} + \eta_2 \psi_2^{-1} + \cdots + \eta_n \psi_n^{-1} \right)}{\sqrt{1 + \eta_2^2 + \cdots + \eta_n^2} \left(\psi_W^{-1} + \psi_1^{-1} + \cdots + \psi_n^{-1} + \mu^{-2} \right) + R \left(\psi_1^{-1} + \eta_2 \psi_2^{-1} + \cdots + \eta_n \psi_n^{-1} \right)}, \tag{21}$$

which shows that $d\mu/dR < 0$ and thus any steady state in which not all x_j are zero (i.e., one or more are strictly positive) can be improved upon by choosing any point, closer to the origin, along the ray connecting this state to the origin. It follows that the optimal steady state is at the origin, that is, μ is maximal when $x_j = 0$ for all j. This steady state with all reserve densities at zero can be characterised as the "lean growth" or "balanced growth" condition (van den Berg, 2001); "lean" because the cells in this state consist entirely of structural components and machinery, "balanced" as re-allocation due by the r-functions effectively "counter-skews" stoichiometric imbalances in the environment (cf. van den Berg et al., 2002).

This lean regulatory regime is optimal only if the environment is unchanging and growth is sufficient, for in that case the steady-state value of μ becomes identical to the fitness ρ as defined by eqn (19), as ultimately $W(t) \sim \exp\{\mu t\}$ or $\ln\{W(t)\}/t \sim \mu$. We can tentatively extend this conclusion to environments that do fluctuate, but remain growth-sufficient in perpetuity: provided that the long-term increase in biomass is not affected too strongly by the transients during which the cells "re-balance" through adaptive re-allocation, μ will be close to the optimum dictated by environmental conditions most of the time. Moreover, steep r-functions (i.e. $\vartheta_j \gg 1$) offer the most reactive response to the changing conditions, minimising the losses that accompany such transients.

4.2. Optimal regulation in a "feast-or-famine" environment

If the environment intermittently imposes conditions which do not support growth at a positive rate (i.e. periods of "famine"), the possibility arises that reserve management is no longer optimal when it is geared to balanced growth, characterised by low ξ_j and high ϑ_j, which promote $x_j \approx 0 \ \forall j$. Whereas these parameter settings maximise fitness in a constant, growth-sufficient environment, as shown in Section 4.1, permitting a certain reserve surplus to build up during times of plenty may allow the organism to maintain growth during times of nutrient shortage. Such a strategy could increase fitness in the sense of eqn (19), in view of the down-time losses incurred when the cell enters a state of metabolic shut-down with zero growth. A cell which maintains reserves close to zero at all times (even during "feast" periods) will spend essentially
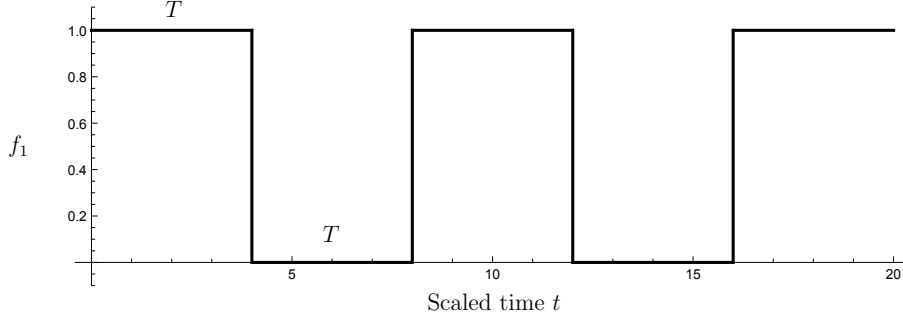
Figure 4: The time-varying environment: a "feast" of duration T alternates with a "famine" also of duration T.

the entire famine period in this shut-down state, in which the metabolic rate has slowed down to virtually zero, and this may depress fitness ρ. The behaviour of the present model as it enters such shut-down states has been treated in detail in a previous paper (Nev and van den Berg, 2017a); essentially, this extreme starved state corresponds to a *sliding mode* of the dynamical system.

To explore this hypothesis, we subject the model, with $n = 1$, to periodic environmental forcing that simulates feast-or-famine conditions in a basic fashion: a piece-wise constant function that alternates between periods of feast ($f_1(t) \equiv 1$) and of famine ($f_1(t) \equiv 0$). Feast and famine both have duration T (in scaled time units); thus the period of the entire cycle is $2T$ (Fig. 4). We set $\zeta_1 = 0$ in the analysis that follows. Numerical results were obtained via simulations performed by means of a stand-alone server application written in *Java 8*. In view of the stiffness properties of the equations, the Gear implicit fourth-order method (Chua and Lin, 1975) was employed to calculate a numerical solution of the system of ODEs. Furthermore, a random-restart hill-climbing approach (Russell and Norvig, 2014) was used to maximise fitness ρ.

Let us first fix $\widehat{r}_1$ and ϑ_1 and consider the variation of the ρ-maximizing value of ξ_1, the midpoint parameter which may be interpreted as the *setpoint* of the reserves, as a function of the environmental parameter T, denoted $\xi_1^*(T)$. As shown in Fig. 5, $\xi_1^*(T)$ is close to zero for both $T \ll 1$ and $T \gg 1$. The non-dimensionalisation of the model is such that the typical time scale of the dynamics is of order 1. Thus the case $T \ll 1$ can be viewed as an environment that fluctuates much more rapidly than the inherent physiological dynamics. The latter effectively average out these fluctuations, and the system behaves as if exposed to a *constant* environment with $f_1 \equiv \frac{1}{2}$ and the results of Section 4.1 can be applied. The case $T \gg 1$ is somewhat more delicate. In this limiting case, the system spends most of its time in the eventual state belonging to the prevailing conditions, i.e. the growth state for $f_1 = 1$ and the sliding mode for $f_1 = 0$. The transients between the two phases become less important as T increases. Thus the fitness ρ is dominated by the biomass gains made during the feast periods, and hence the optimal parameter regime accords with the results of Section 4.1. This leaves the intermediate case where $T \sim 1$. Here transient dynamical behaviour following the changes in environmental conditions dominates the outcome. These transients are associated with the depletion of reserves during famines and reserve replenishment during feasts. The optimal reserve level $\xi_1^*(T)$ appears to be such that the reserve density just attains the sliding mode at the end of the feast period.
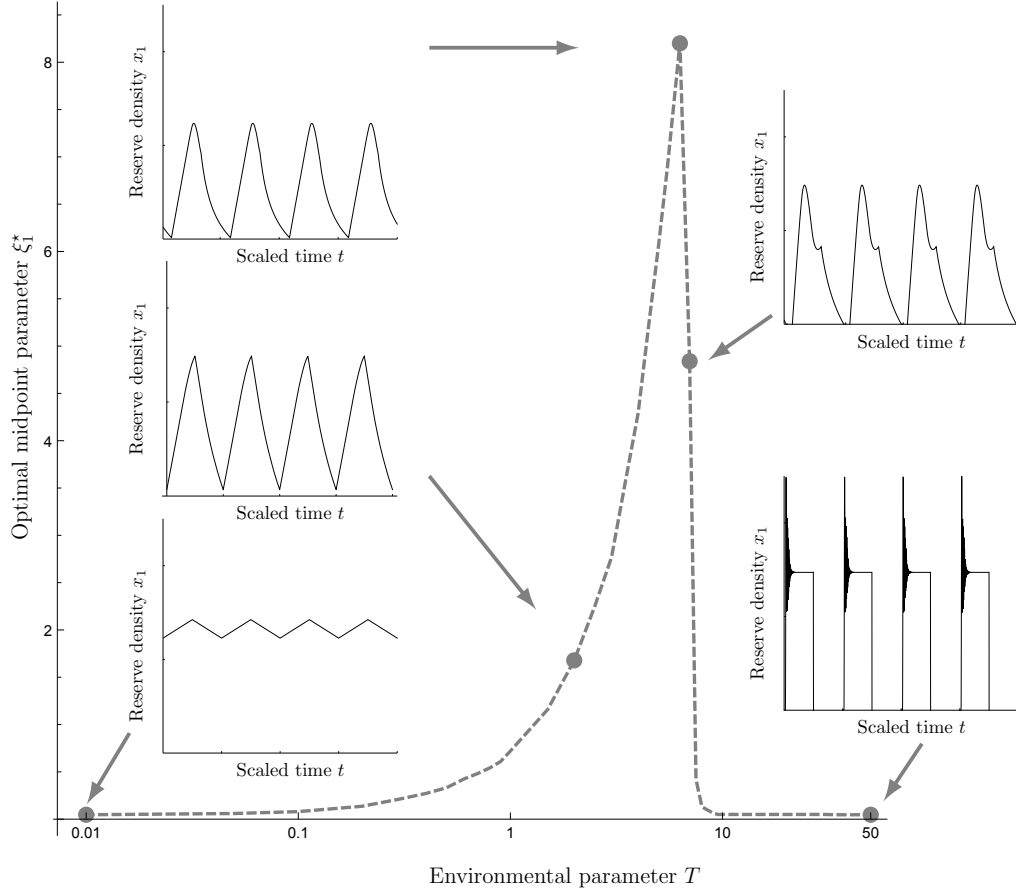
Figure 5: Fitness-optimal midpoint shape parameter $\xi_1^*(T)$ of the regulatory function $r_1(x_1)$ as a function of the environmental parameter T. Insets show each four stationary cycles at the optimal parameter value; the abscissa thus has width $8T$ and the ordinate runs from 0 to $2.5\times$ the optimal value $\xi_1^*(T)$. The parameter $\widehat{r}_1$ was fixed at the value 10 and the parameter ϑ_1 was fixed at the value 100.

Next, we fix $\widehat{r}_1$ and ξ_1 and consider the variation of the ρ-maximizing value of ϑ_1, the steepness parameter which may be interpreted as the *regulatory reactivity* of the control system, as a function of the environmental parameter T, denoted $\vartheta_1^*(T)$. Again we can observe agreement with the results of Section 4.1 in the cases $T \ll 1$ and $T \gg 1$, with much reduced optimal steepness in the intermediate case $T \approx 7$ (Fig. 6). This lower value of $\vartheta_1^*(T)$ allows for a greater amplitude of reserve density fluctuation over the stationary cycle, again with the reserve density just attaining the sliding mode at the end of the feast period.

More generally, we should treat ρ as a function of the three parameters $\{\xi_1, \vartheta_1, \widehat{r}_1\}$. The latter variable, $\widehat{r}_1$, is fitness-limiting when it is too small, since the operating range of the control system is then constrained by this variable; for $\widehat{r}_1 \gg 10$, optimal fitness ρ becomes insensitive to this parameter. Accordingly, we fix $\widehat{r}_1$ at the sufficiently large value 10 and determine the maximum fitness ρ with respect to ξ_1 and ϑ_1. We observe that the optimal stationary cycles again display the greatest variation in reserve density x_1 for $T \approx 6$, with smaller amplitude variations for both
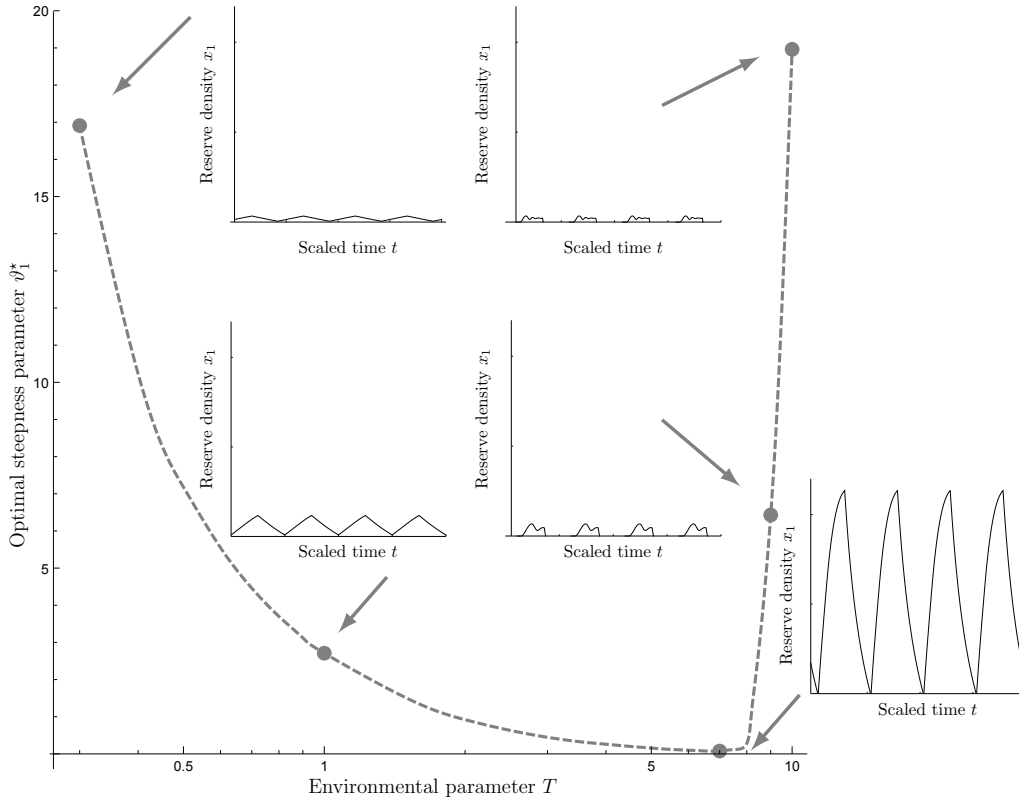
Figure 6: Fitness-optimal steepness parameter $\vartheta_1^*(T)$ of the regulatory function $r_1(x_1)$ as a function of the environmental parameter T. Insets each show four stationary cycles at the optimal parameter value; the abscissa thus has width $8T$ and the ordinate runs from 0 to 12. The parameter $\widehat{r}_1$ was fixed at the value 10 and the parameter ξ_1 was fixed at the value 0.1.

$T \ll 1$ and $T \gg 1$ (Fig. 7). For large T, the sliding mode behaviour at the end of famine intervals can be seen. The optimal r-functions, shown in the insets of Fig. 7, exhibit a 2- to 3-fold variation of r_1 over the stationary cycle for the intermediate regime, with a greater variation at the extremes ($T \ll 1$, $T \gg 1$).

5. Discussion

Intracellular reserves, also known as variable internal stores (Grover, 1991) are a conspicuous feature of microbial organisms, sometimes occupying a significant portion of the volume of the cell and often present in the form of inclusion bodies (Beveridge, 1989; Preiss, 1989; Dawes, 1989). Our results suggest that we should expect to find such features predominantly in fluctuating environments, since the optimal management strategy regarding reserves in stable growth-supporting environments is to maintain minimal reserve densities. Moreover, the time scale of the environmental fluctuations is important: very rapid fluctuations are irrelevant, and very slow fluctuations are essentially equivalent to constant environments, since stores that would allow the cells to tide them over the entire famine period would have to be unfeasibly

14
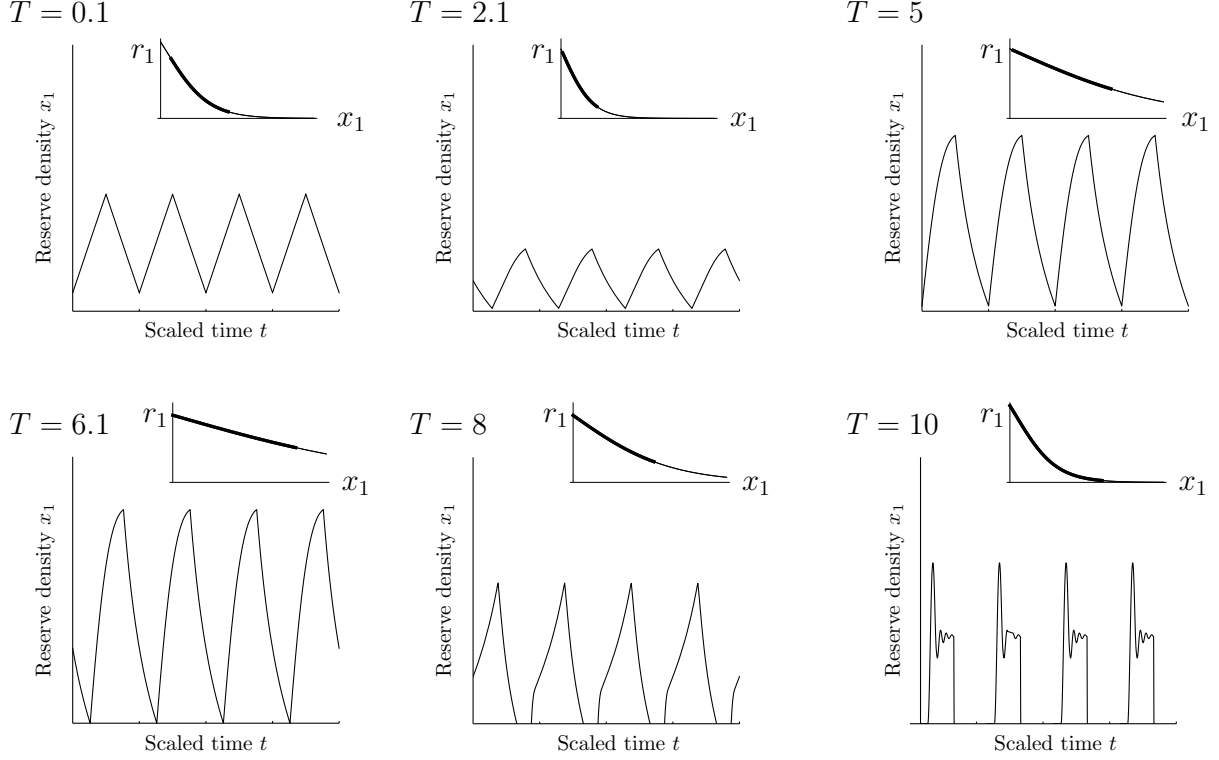
Figure 7: Stationary cycles for fitness-optimal r-functions. Each panel shows four stationary cycles of the reserve density, total duration $8T$ with T as indicated, with ordinate running from 0 to 0.25 for $T = 0.1$ and $T = 10$ and 12 for all other values of T. The parameter $\widehat{r}_1$ was fixed at the value 10 and the parameters ξ_1 and ϑ_1 were simultaneously optimised for maximal ρ. Insets show the corresponding optimal r-functions, with abscissa running from 0 to 0.25 for $T = 0.1$ and $T = 10$ and 12 for all other values of T and ordinate from 0 to 6 in all cases. The heavy-lined portion of the inset graphs corresponds to the working range of the stationary cycle.

large, and thus such periods become dead losses. Thus optimal reserve management is governed primarily by fluctuations that happen at a time scale comparable to that of the cell's physiology; this might be termed "eco-physiological resonance." An important consideration in looking for evidence of such eco-physiological resonance in real-life ecosystems is that the intrinsic time scale of the organism determines the timescale of ecological fluctuations on which such resonance should be expected: these intrinsic time scales vary over several orders of magnitude; for instance, doubling times in microbial habitats range from 10 min in hydrothermal vents in freshwater lakes (Elsgaard and Prieur, 2011) to thousands of years in deep-sea beds (Jørgensen and Boetius, 2007).

At the height of this eco-physiological resonance regime, the optimal parameter setting appears to be such that the stores just suffice to tide the cell over. In other words, the system reaches the sliding-mode regime just as the next feast period commences. This observation is in keeping with the results obtained by Parnas and Cohen (1976) who used a similar, if slightly more coarse-grained, model of macro-chemical kinetics.

The limitations and possible extensions of the present study are readily apparent if we con-

sider the more general definition of fitness proposed by Metz et al. (1992): the fitness of a given type Y is the asymptotic exponential growth rate $\rho_{E(C)}(Y)$ of the biomass of Y in an ergodic environment E in which the type is present in vanishingly small proportions relative to resident types $C \equiv \{X_1, \ldots, X_n\}$. This definition implies that $\rho_{E(C)}(X_i) = 0$ for $i = 1, \ldots, n$, since the biomasses of resident types cannot go to zero (this is what it means to be *resident*; so $\rho_{E(C)}(X_i) < 0$ is ruled out) and none of those masses can go to infinity either (so $\rho_{E(C)}(X_i) > 0$ is ruled out as well). By contrast, for the non-resident type Y, interest centres on the case $\rho_{E(C)}(Y) > 0$ since its extinction is otherwise assured. The definition we have employed, eqn (19), accords for the particular eco-evolutionary scenario we have studied with the general one, but the latter encompasses *ergodic environments* and *multiple (competing, mutant) types*.

As regards the general presence of multiple competing eco-types, what we have studied here is optimality of reserve management *tout court*, as it were from an engineering perspective, isolating the role of reserves as stored supplies for times of scarcity. The presence of variant types in the environment would complicate the analysis since another role of reserves would come into play, namely that of capturing nutrients before a competitor can: short-term rapid uptake of peaks in ambient availability may then become a major factor.

Moreover, the spatial ordering of the environment may be important in how these competitive effects are transmitted. In a well-mixed environment, such as a high-turbidity lake, cells may be expected to be exposed to competing type cells *pro rata*, but by the same token, the effects are averaged out as the nutrient concentration tends to be uniform across the ecological system. By contrast, in a more static diffusion-limited environment, such as a biofilm-like system (cf. van Gemerden, 1993), most cells may be surrounded by cells of like type, and competition is confined to the interfaces between subpopulations, which may allow polymorphisms to persist which would otherwise not be available (e.g., Grover et al., 2012).

As regards ergodic environments, the deterministic alteration studied here, with fixed time scale T, can be generalised to stochastic environments in which the duration of a feast or a famine is realised from a suitable statistical distribution, such as a Gaussian or exponential distribution. (In more advanced variations, the level f could itself be treated as a random variable, but still piecewise constant, or alternatively $f(t)$ could be the subject of an SDE.) We surmise that the present results would still go through in a qualitative sense. In particular, the average duration of a famine would have to be order 1 to evoke ξ_1^* bounded away from zero, as a consequence of the eco-physiological resonance effect described above, but the effect would be tempered by the extent to which feast periods allow the requisite storage levels to accumulate; if the feasts are relatively short, we do not expect the stores at the start of a typical famine period to be sufficient to keep the model away from the sliding mode for the entire duration of that famine. On the other hand, we do not expect long feast periods to negate the need to accumulate stores (cf. Parnas and Cohen, 1976).

Of special interest is the extension to stochastic (ergodic) environments for multiple nutrient limitation (i.e. the case $n > 1$). Let us consider the simplest version of such a model, in which each of the n environmental factors f_j can occur in either the state 0 or 1. Thus 2^n distinct joint environmental states are possible, and the transitions between these states can be described as a continuous-time Markov chain. The key quantity in this setting is the correlation between the feast states for the various factors (and thus also between the famine states). We conjecture

16

that negative correlation would result in higher reserve "setpoints" ξ_j. For instance, for $n = 2$, strong negative correlation would imply that at most points in time, one is high while the other is low, with strict alternation between which one is feast and which is famine. In that case the storage serves not so much to survive times of scarcity, but to carry on growing while only one factor is readily available. In contrast to the "survival" aspect which is associated with providing energy to sustain the needs of endogenous metabolism, this second role is also important with regard to building blocks (e.g., N, P, S, trace metals,...). Strong positive correlation, on the other hand, would effectively reduce the dimensionality of the model back to $n = 1$, as the various environmental factors behave as though they were a single, more complex, nutrient compound. To conclude our conjecture on correlation, we surmise that eco-physiological resonance would be negated, or only possible for a limited range of environmental parameter values, as n increases when there is weak or no correlation between the environmental factors.

In terms of physiological realism, the present model implicitly assumes that the pool of core intermediary metabolites is kept under strict homeostasis; this assumption allows the rates of synthesis of macromolecules to be treated as acceptor-driven. By contrast, a detailed *micro-chemical* approach would account explicitly for constraints on rates of reaction arising both from donors (reactants) and acceptors (products) in these reactions. Specifically, the connection between such a micro-chemical approach and the present macro-chemical approach is as follows. Let $\boldsymbol{S}$ denote the stoichiometric matrix accounting for all biochemical species present in the organism; $\boldsymbol{S}$ has as many rows as there are chemical elements involved and as many columns as there are chemical species (i.e. the columns are [empirical] formulas). A reaction can be represented as a *reaction stoichiometry* $\boldsymbol{v}$, a vector whose elements are reaction coefficients (negative for reactants, positive for products, zero for species neither created nor destroyed) and which must satisfy $\boldsymbol{S} \cdot \boldsymbol{v} = \boldsymbol{0}$ since atoms undergo neither creation nor destruction or transmutation during chemical reactions, so that a valid $\boldsymbol{v}$ can be written as a linear combination of a given basis of Nul $\boldsymbol{S}$—if we choose a basis for Nul $\boldsymbol{S}$ and let the basis vectors be the columns of $\boldsymbol{B}$, the rth reaction stoichiometry $\boldsymbol{v}_r$ can be written as $\boldsymbol{B} \cdot \boldsymbol{\kappa}_r$, with dim $\boldsymbol{\kappa}_r =$ dim Nul $\boldsymbol{S}$. Moreover, if $\dot{v}_r$ is the rate at which the rth reaction proceeds, the net exchange flux can be written as $\sum_r \boldsymbol{v}_r \dot{v}_r = \sum_r \boldsymbol{B} \cdot \boldsymbol{\kappa}_r \dot{v}_r = \boldsymbol{B} \cdot \dot{\boldsymbol{\xi}}$. Since the number of biochemical species in a biological cell is considerable and the number of distinct biogenic chemical elements is modest, dim Nul $\boldsymbol{S}$ will be sizable (even if $\boldsymbol{S}$ is full-rank, as is usually the case), and this would suggest that $\dot{\boldsymbol{\xi}}$ is quite high-dimensional. However, $\dot{\boldsymbol{\xi}}$ is subject to homeostatic constraints. In particular, let the columns of the compositional superposition matrix $\boldsymbol{H}$ describe the macro-chemical components (i.e., in the notation of the present paper, $M_0, \ldots, M_n, M_G, W$) in terms of their constituent biochemical species, and append to $\boldsymbol{H}$ standard units vectors picking out the small-molecular reactants assimilated or dissimilated from the ambient medium (nutrients, redox substrates), of the products appearing in the medium (excreta, redox products), with signs adapted to the macro-chemical components. Thus $\boldsymbol{H}$ has as many rows as there are biochemical species and as many columns as there are components plus chemical species involved in the cell's interactions with the ambient. Then $\boldsymbol{B} \cdot \dot{\boldsymbol{\xi}} = \boldsymbol{H} \cdot \dot{\boldsymbol{\vartheta}}$ where $\dot{\boldsymbol{\vartheta}}$ is a macro-chemical rate vector (van den Berg, 2011, p. 112). Now $\dot{\boldsymbol{\vartheta}}$ is constrained by quantities such as $\widetilde{\hat{\phi}}_j$ and f_i which in turn depend on expression levels of the catalytic machinery mediating these fluxes, as well as ambient conditions (such as nutrient concentrations). On the present

approach, specification of $\boldsymbol{\mathring{\vartheta}}$ is completed by choosing the r-functions. Fixing $\boldsymbol{\mathring{\vartheta}}$ enforces a reduction in degrees of freedom; the number of remaining degrees of freedom is given by:

$$\mathrm{df} = \mathrm{dim}\ \mathrm{Nul}\ [-\boldsymbol{H} \mid \boldsymbol{B}] - \mathrm{dim}\ \boldsymbol{\mathring{\vartheta}}\ . \tag{22}$$

The requirement of consistency of the macro-chemical description with the micro-chemical substratum is expressed by $\mathrm{df} \geq 0$. Finally, to fix the individual reaction rates $\mathring{v}_r$, we must adduce additional conditions, such as expression levels of individual enzymes (these constrain the rates $\mathring{v}_r$ which are linked by $\boldsymbol{\dot{\xi}} = \sum_r \boldsymbol{\kappa}_r \mathring{v}_r$) and, for instance, the desideratum that μ is to be maximised. This has been carried out in impressive detail by Palsson and co-workers (Orth et al., 2010; O'Brien et al., 2013), who effectively assumed constant ratios between the components $M_0, \ldots, M_n, M_G, W$; extending their analysis to the case where this latter assumption is relaxed should be relatively straightforward.

   The assumption of acceptor-driven kinetics, which is implicit in the equations of Section 2, breaks down under metabolic shutdown conditions, which means that under such conditions the macro-chemical model could be extended with explicit donor-controlled rate multipliers, or equivalently, as we have shown elsewhere (Nev and van den Berg, 2017a), by postulating a sliding mode for the dynamics. The model is based on $n+1$ feedback loops, one between each reserve density and the allocation of molecular building blocks towards the machinery dedicated to the assimilation of that nutrient, in addition to a basic growth-control loop that is based on homeostasis of the density of synthetic (zero-type, i.e. machinery-making) machinery; the latter may be referred to as the M_0/M_G-loop. This logic is similar to that proposed by Scott and co-workers (Scott et al., 2010; Scott and Hwa, 2011; Scott et al., 2014). The nutrient loops are expressed by the r-functions reconstructed from experimental data in Section 3, whereas the M_0/M_G-loop is consistent with the findings by Herbert (1961). In its present form, all nutrients are treated as essential; when nutrients can be exchanged for one another, the phenomenon of metabolic switching must be taken into account, and the regulatory laws become more involved than the ones considered here. Finally, we have not taken into account here the possibility of endogenous rhythmic processes, which may supply important timing cues to the control system. Such processes would effectively serve as clocks that govern several of the parameters of the r-functions.

References

Beveridge, T. J., 1989. The structure of bacteria. In: Poindexter, J. S., Leadbetter, E. R. (Eds.), Bacteria in Nature III: Structure, Physiology, and Genetic Adaptability. Plenum, pp. 1–65.

Bremer, H., Dennis, P. P., 1996. Modulation of chemical composition and other parameters of the cell by growth rate. In: Neidhardt, F., et al. (Eds.), *Escherichia coli* and *Salmonella typhimurium*: Cellular and Molecular Biology. ASM Press, Ch. 97.

Chua, L. O., Lin, P.-M., 1975. Computer-aided analysis of electronic circuits: Algorithms and computational techniques. Prentice-Hall.

Dawes, E. A., 1989. Growth and survival of bacteria. In: Poindexter, J. S., Leadbetter, E. R. (Eds.), Bacteria in Nature III: Structure, Physiology, and Genetic Adaptability. Plenum, pp. 67–187.

Dortch, Q., Clayton, J. R., Thoresen, S. S., Ahmed, S. I., 1984. Species differences in accumulation of nitrogen pools in phytoplankton. Marine Biology 81, 237–250.

Doudoroff, M., Stanier, R. Y., 1959. Role of poly-β-hydroxybutyric acid in the assimilation of organic carbon by bacteria. Nature, Lond. 183, 1440–1442.

Droop, M. R., 1968. Vitamin B12 and marine ecology. IV. The kinetics of uptake, growth and inhibition in *Monochrysis lutheri*. J. Mar. Biol. Assoc. 48, 689–733.

Elsgaard, L., Prieur, D., 2011. Hydrothermal vents in Lake Tanganyika harbor spore-forming thermophiles with extremely rapid growth. J. Great Lakes Res. 37, 203–206.

Grover, J. P., 1991. Resource competition in a variable environment: Phytoplankton growing according to the Variable-Internal-Stores model. Amer. Nat. 138, 811–835.

Grover, J. P., Hsu, S.-B., Wang, F.-B., 2012. Competition between microorganisms for a single limiting resource with cell quota structure and spatial variation. J. Math. Biol. 64, 713–743.

Harrison, P. J., Conway, H. L., Dugdale, R. C., 1976. Marine diatoms grown in chemostats under silicate or ammonium limitation. I. Cellular chemical composition and steady-state growth kinetics of *Skeletonema costatum*. Mar. Biol. 35, 19–31.

Henry, N. G., 1969. Effect of decreasing growth temperature on cell yield of *Escherichia coli*. J. Bacteriol. 98, 232–237.

Herbert, D., 1958. Some principles of continuous culture. In: Tunevall, G. (Ed.), Recent Progress in Microbiology. Almquist & Wiksell, Stockholm, pp. 381–396.

Herbert, D., 1961. The chemical composition of micro-organisms as a function of their environment. Symp. Soc. Gen. Microbiol. 11, 391–416.

Holme, T., Palmstierna, H., 1956. Changes in glycogen and nitrogen-containing compounds in *Escherichia coli* B during growth in deficient media. I. nitrogen and carbon starvation. Acta. Chem. Scand. 10, 578–586.

Jørgensen, B. B., Boetius, A., 2007. Feast and famine – microbial life in the deep-sea bed. Nat. Rev.. Microbiol. 5, 770–781.

Kramer, G., Sprenger, R. R., Nessen, M. A., Roseboom, W., Speijer, D., de Jong, L., Texeira de Mattos, M. J., Back, J., de Koster, C. G., 2010. Proteome-wide alterations in *Escherichia coli* translation rates upon anaerobiosis. Mol. Cell. Proteomics 9.11, 2508–2516.

Lenski, R. E., Rose, M. R., Simpson, S. C., Tadler, S. C., 1991. Long-term experimental evolution in *Escherichia coli*. I. Adaptation and divergence during 2,000 generations. Amer. Nat. 138, 1315–1341.

Liebermeister, W., Noor, E., Flamholz, A., Davidi, D., Bernhardt, J., Milo, R., 2014. Visual account of protein investment in cellular functions. Proc. Natl. Acad. Sci. U.S.A. 111, 8488–8493.

Marr, A. G., Nilson, E. H., Clark, D. J., 1962. The maintenance requirement of *Escherichia coli*. Ann. N. Y. Acad. Sci 102, 536–548.

Metz, J. A. J., Meszena, S. A. H., Jacobs, F. J. A., van Heerwaarden, J., 1995. Adaptive dynamics: A geometrical study of the consequences of nearly faithful reproduction. Tech. Rep. WP-95-099, IIASA, Laxenburg, Austria.

Metz, J. A. J., Nisbet, R. M., Geritz, S. A. H., 1992. How should we define 'fitness' for general ecological scenarios? TRENDS in Ecology & Evolution 7, 198–202.

Neidhardt, F. C., Ingraham, J. L., Schaechter, M., 1990. Physiology of the Bacterial Cell: A Molecular Approach. Sinauer Associates, Sunderland.

Nesmeyanova, M. A., 2000. Polyphosphates and enzymes of polyphosphate metabolism in *Escherichia coli*. Biochemistry (Moscow) 65, 309–314.

Nev, O. A., van den Berg, H. A., 2017a. Microbial metabolism and growth under conditions of starvation modelled as the sliding mode of a differential inclusion. Dyn. Systems *in press*.

Nev, O. A., van den Berg, H. A., 2017b. Variable-Internal-Stores models of microbial growth and metabolism with dynamic allocation of cellular resources. J. Math. Biol. 74, 409–445.

Noguchi, Y., Nakai, Y., Shimba, N., Toyosaki, H., Kawahara, Y., Sugimoto, S., Suzuki, E., 2004. The energetic conversion competence of *Escherichia coli* during aerobic respiration studied by ^{31}P NMR using a circulating fermentation system. J. Biochem. 136, 509–515.

O'Brien, E. J., Lerman, J. A., Chang, R. L., Hyduke, D. R., Palsson, B. O., 2013. Genome-scale models of metabolism and gene expression extend and refine growth phenotype prediction. Mol. Syst. Biol. 9, a693.

Orth, J. D., Thiele, I., Palsson, B. O., 2010. What is flux balance analysis? Nat. Biotechnol. 28, 245–248.

Pan, S., Shen, Z., Liu, W., Han, X., Miao, H., Ma, H., 2010. Nutrient compositions of cultured *Skeletonema costatum*, *Chaetoceros curvisetus*, and *Thalassiosira nordenskiöldii*. Chinese J. Oceanol. Limnol. 28, 1131–1138.

Parnas, H., Cohen, D., 1976. The optimal strategy for the metabolism of reserve materials in micro-organisms. J. Theor. Biol. 56, 19–55.

Pirt, S. J., 1965. The maintenance energy of bacteria in growing cultures. Proc. Roy. Soc. Lond. 133, 300–302.

Preiss, J., 1989. Biochemistry and metabolism of intracellular reserves. In: Poindexter, J. S., Leadbetter, E. R. (Eds.), Bacteria in Nature III: Structure, Physiology, and Genetic Adaptability. Plenum, pp. 189–258.

Rhee, G.-Y., 1973. A continuous culture study of phosphate uptake, growth rate and polyphosphate in *Scenedesmus sp.* J. Phycol. 9, 495–506.

Rich, P. R., 2003. The molecular machinery of Keilin's respiratory chain. Biochem. Soc. Trans., 1095–1105.

Riley, M., Abe, T., Arnaud, M. B., Berlyn, M. K., Blattner, F. R., Chaudhuri, R. R., Glasner, J. D., Horiuchi, T., Keseler, I. M., Kosuge, T., Mori, H., Perna, N. T., Plunkett, G., Rudd, K. E., Serres, M. H., Thomas, G. H., Thomson, N. R., Wishart, D., Wanner, B. L., 2006. *Escherichia coli* K-12: A cooperatively developed annotation snapshot2005. Nucleic Acids Res. 34, 1–9.

Russell, S. J., Norvig, P., 2014. Artificial Intelligence: A Modern Approach, 3rd Edition. Upper Saddle River : Prentice Hall.

Schulze, K. L., Lipe, R. S., 1964. Relationship between substrate concentration, growth rate, and respiration rate of *Escherichia coli* in continuous culture. Arch. Microbiol. 48, 1–20.

Scott, M., Gunderson, C. W., Mateescu, E. M., Zhang, Z., Hwa, T., 2010. Interdependence of cell growth and gene expression: Origins and consequences. Science 330, 1099–1102.

Scott, M., Hwa, T., 2011. Bacterial growth laws and their applications. Curr. Opinion Biotechnol. 22, 599–565.

Scott, M., Klumpp, S., Mateescu, E. M., Hwa, T., 2014. Emergence of robust growth laws from optimal regulation of ribosome synthesis. Mol. Syst. Biol. 10, 747.

Sweetman, A. J., Griffiths, D. E., 1971. Studies on energy-linked reactions. Energy-linked transhydrogenase reaction in *Escherichia coli*. Biochem. J. 121, 125–130.

Valgepea, K., Adamberg, K., Seiman, A., Vilu, R., 2013. *Escherichia coli* achieves faster growth by increasing catalytic and translation rates of proteins. Mol. Biosyst. 9, 2344–2358.

van den Berg, H. A., 2001. How microbes can achieve balanced growth in a fluctuating environment. Acta Biotheor. 49, 1–21.

van den Berg, H. A., 2011. Mathematical Models of Biological Systems. Oxford University Press.

van den Berg, H. A., 2015. Evolutionary Dynamics: The Mathematics of Genes and Traits. Institute of Physics.

van den Berg, H. A., Kiselev, Y. N., Orlov, 2002. Optimal allocation of building blocks between nutrient uptake systems in a microbe. J. Math. Biol. 44, 276–296.

van den Berg, H. A., Orlov, M., Kiselev, Y. N., 2008. The Malthusian parameter in microbial ecology and evolution: An optimal control treatment. Comp. Math. Model. 19, 406–428.

van Gemerden, H., 1993. Microbial mats: A joint venture. Mar. Geol. 113, 3–25.

West, G. S., 1916. Algae. Volume 1, Myxophyceae, Peridinieae, Bacillarieae, Chlorophyceae. Cambridge University Press, Cambridge.

Williams, F. M., 1967. A model of cell growth dynamics. J. Theor. Biol. 15, 190–207.

Yuan, J., Fowler, W. U., Kimball, E., Lu, W., Rabinowitz, J. D., 2006. Kinetic flux profiling of nitrogen assimilation in *Escherichia coli*. Nat. Chem. Biol. 2, 529–530.

Appendix A. Stoichiometric calculations and estimates

A wealth of data is available for the species *Escherichia coli*, which we will here take as our model for a "typical" prokaryotic cell, using these data to estimate the various stoichiometric parameters.

Appendix A.1. Assignment of proteins to components

The first step is to assign the proteins expressed, or potentially expressed, by an *E. coli* cell to the macro-chemical components as distinguished within the context of the mathematical model described in Section 2. Proteins dedicated to transcription and translation are shared between the machinery that generates catalytic machinery (i.e., the macro-chemical component denoted M_0) and the machinery that generates more structural biomass (i.e., machinery M_G generating structural biomass W), since both types of machinery produce proteins. In addition, the machinery for growth M_G comprises proteins involved in the synthesis of the cell envelope, proteins involved in DNA replication and cell division, genomic maintenance and duplication, as well as biosynthetic pathways. Uptake machinery (denotes $M_1, \ldots, M_n$) comprises proteins that underlie the assimilation of nutrients from the ambient environment, such as transporters and binding proteins, as well as the machinery required to transform these nutrients into core metabolites. Guided by these general principles, we obtain the assignment of all currently known and functionally identified *E. coli* proteins to components, as detailed in Table A.2. Valgepea et al. (2013) give quantitative estimates for the cellular abundance of each of these proteins. Summing the totals for each component, we find that the structural component (W) accounts for $\sim 39.4\%$ of the protein dry weight, synthetic machinery (M_0) for $\sim 19.6\%$, growth machinery (M_G) for $\sim 33.8\%$, and assimilatory (or "uptake") machinery ($M_1, \ldots, M_n$) for $\sim 7.2\%$. Among the latter, machinery devoted to the assimilation of glucose, nitrogen, and phosphorus, accounting for, respectively, 0.563%, 0.44%, and 0.1% of the total cellular protein mass.

The structural component W comprises $\sim 39.4\%$ of the protein mass, which means that the fraction of RNA- and ribosome-related proteins belonging to the growth machinery is about 0.394,

22

since the growth machinery is dedicated to the synthesis of the structural component. It follows that machinery M_0 synthesising catalytic machinery accounts for $\sim 60.6\%$ of all RNA- and ribosome-related proteins in the cell. Let $\beta_0 = 0.606$ denote the portion of RNA- and ribosome-related proteins that appertain to the synthetic machinery, and $1 - \beta_0 = 0.394$ for the remainder.

Assuming equal protein sizes on average across the components, we can convert these estimates into allocation coefficients, as follows:

$$\alpha_0 = 0.323, \quad \alpha_G = 0.558, \quad \alpha_{\text{Gl}} = 0.0093, \quad \alpha_{\text{N}} = 0.0073, \quad \alpha_{\text{P}} = 0.0017, \qquad \text{(A.1)}$$

where the subscripts Gl, N, and P stand for glucose, nitrogen, and phosphorus, respectively.

According to Neidhardt et al. (1990), one gram of *E. coli* contains 0.55 g of protein and 0.2053 g RNA. This gives

$$0.55 \times 0.196 + 0.2053 \times \beta_0 = 0.232 \text{ g synthetic machinery per gram-cell;}$$
$$0.55 \times 0.338 + 0.2053 \times (1 - \beta_0) = 0.267 \text{ g growth machinery per gram-cell;}$$
$$0.55 \times 0.072 = 0.0396 \text{ g assimilatory machinery per gram-cell.}$$

The structural component comprises every molecule not assigned to catalytic machinery or reserves; the latter comprise ~ 0.025 g per gram-cell (Neidhardt et al., 1990). Thus, by subtraction, we have

$$1 - (0.232 + 0.267 + 0.0396 + 0.025) = 0.436 \text{ g structural component per gram-cell.}$$

Appendix A.2. Rates of production

Protein elongation. The rate of elongation attained by a single ribosome is 18 amino acids per second (Bremer and Dennis, 1996); multiplying this by the total of $\sim 26{,}300$ ribosomes per cell (Bremer and Dennis, 1996), we have for the whole-cell protein synthesis elongation rate:

$$18 \times 26{,}300 = 473{,}400 \text{ amino acids per second per cell.}$$

Equivalently, using a dry weight of one cell of $\sim 2.8 \times 10^{-13}$ grams (Neidhardt et al., 1990),

$$473{,}400/(2.8 \times 10^{-13}) = 1{,}690.7 \times 10^{15} \text{ amino acids/(s·gram-cell).}$$

With 550 mg of protein, equivalent to $5{,}081 \times 10^{-6}$ mol amino acid residues, for every gram-cell (Neidhardt et al., 1990), we finally calculate

$$1{,}690.7 \times 10^{15} \times 550 \times 10^{-3}/(5{,}081 \times 10^{-6} \times N_A) =$$

$$0.0003039 \text{ g protein/(s·gram-cell)},$$

where $N_A = 6.02214129 \times 10^{23}$.

Scaled parameters. Using eqn (A.1) and the value of β_0, we can now calculate estimates for the stoichiometric coefficients $\widetilde{\phi}_k$ from eqn (1), which express the rate of production of the machinery of type k:

$$\widetilde{\phi}_0 = \frac{0.0003039 \times \beta_0 \times (1 + \text{g RNA in } M_0/\text{g of proteins in } M_0)}{\alpha_0 \times \text{g of } M_0} =$$

$$\frac{0.0003039 \times \beta_0 \times (1 + 0.124/0.108)}{0.323 \times 0.232} = 0.0053 \text{ per second },$$

$$\widetilde{\phi}_G = \frac{0.0003039 \times \beta_0 \times (1 + \text{g RNA in } M_G/\text{g of proteins in } M_G)}{\alpha_G \times \text{g of } M_0} =$$

$$\frac{0.0003039 \times \beta_0 \times (1 + 0.081/0.186)}{0.558 \times 0.232} = 0.002 \text{ per second },$$

$$\widetilde{\phi}_{Gl} = \frac{0.0003039 \times \beta_0}{\alpha_{Gl} \times \text{g of } M_0} = \frac{0.0003039 \times \beta_0}{0.0093 \times 0.232} = 0.085 \text{ per second },$$

$$\widetilde{\phi}_N = \frac{0.0003039 \times \beta_0}{\alpha_N \times \text{g of } M_0} = \frac{0.0003039 \times \beta_0}{0.0073 \times 0.232} = 0.109 \text{ per second },$$

$$\widetilde{\phi}_P = \frac{0.0003039 \times \beta_0}{\alpha_P \times \text{g of } M_0} = \frac{0.0003039 \times \beta_0}{0.0017 \times 0.232} = 0.5 \text{ per second }.$$

The specific growth rate prior to scaling $\widetilde{\mu}$ is equal to $\frac{d}{dt} \ln W(t) \equiv \dot{W}/W$ by definition where $\dot{W} = \widetilde{\psi}_W M_G$ in the present model. Over a period of time in which $\widetilde{\mu}$ is not time-varying, this parameter is related to the doubling time $\widetilde{T}_2$ by the formula $\widetilde{\mu} = \ln\{2\}/\widetilde{T}_2$. Hence, using $\widetilde{T}_2 = 2,400$ sec (Neidhardt et al., 1990), we have $\widetilde{\mu} = 0.00029 \text{ sec}^{-1}$, which leads us to

$$\widetilde{\psi}_W = \frac{\widetilde{\mu}}{M_G/W} = \frac{0.00029 \text{ per second}}{0.267 \text{ g } M_G \text{ per gram-cell}/0.436 \text{ g } W \text{ per gram-cell}} = 0.00047 \text{ per second }.$$

Applying the scaling, eqn (5), and considering the cell in homeostasis for synthetic machinery (i.e., $m_0 = 1 \Leftrightarrow M_0/W = \hat{m}$), we obtain:

$$\psi_W = \frac{\widetilde{\psi}_W \widetilde{\phi}_G}{\widetilde{\phi}_0^2} \hat{m} = \frac{\widetilde{\psi}_W \widetilde{\phi}_G}{\widetilde{\phi}_0^2} \frac{M_0}{W} =$$

$$\frac{0.00047 \text{ per s} \times 0.002 \text{ per s}}{0.0053^2 \text{ per s}^2} \times \frac{0.232 \text{ g of } M_0 \text{ per gram-cell}}{0.436 \text{ g of } W \text{ per gram-cell}} = 0.018 .$$

Appendix A.3. Stoichiometric coefficients related to glucose

Glucose as a building block. Neidhardt et al. (1990) indicate that *E. coli* is 50% carbon by dry weight (d/w). Since glucose ($C_6H_{12}O_6$, molar mass 180 g/mol) is the only source of carbon for *E. coli* when grown in a minimal medium, it follows that one gram of cell d/w requires $0.5 \times 180/(12 \times 6) = 1.25$ g of glucose (i.e. $180/(12 \times 6) = 2.5$ g glucose is required for each g C). Protein per g d/w requires 0.29 g of carbon (Neidhardt et al., 1990); therefore protein synthesis requires

0.29 g of C per gram-cell $\times$ 2.5 g glucose per g of C = 0.73 g glucose per gram-cell ,

24

since we consider the glucose to be the sole source of carbon. RNA requires 0.072 g of carbon per gram-cell (Neidhardt et al., 1990), and thus

0.072 g C per gram-cell × 2.5 g glucose per g C = 0.18 g glucose per gram-cell

is required for RNA synthesis. According to Neidhardt et al. (1990), glycogen (the main glucose reserve in the cell of *E. coli*) accounts for 0.028 g glucose per gram-cell, and the energetic cost of forming the glycogen polymer out of glucose is negligible.

Glucose as a source of energy. The maximum ATP yield per molecule of glucose is ~ 29.38 ATP molecules (Rich, 2003), thus $1/29.38 = 0.034$ molecules of glucose must be completely catabolised to produce one molecule of ATP. The total energy required for polymerisation of all essential macromolecules to create one gram d/w equals 0.023 mol ATP per gram-cell (Neidhardt et al., 1990); accordingly, the energetic requirement to render all macromolecules in their polymeric form is

0.023 mol ATP per gram-cell × 0.034 molecules of glucose per molecule ATP × 180 g/mol =
0.14 g glucose per gram-cell .

In terms of protein synthesis, 0.022 mol ATP per g d/w is required to drive the processes of activation and incorporation, as well as to provide the cell with the energy for proofreading, assembly, and modification reactions (Neidhardt et al., 1990). This is equivalent to

0.022 mol ATP per gram-cell × 0.034 molecules of glucose per molecule ATP × 180 g/mol =
0.13 g glucose per gram-cell .

In terms of RNA synthesis, a similar calculation yields:

0.00026 mol ATP per gram-cell × 0.034 molecules of glucose per molecule ATP × 180 g/mol =
0.0016 g glucose per gram-cell .

In addition, glucose must be expended to fuel the synthesis of the monomeric building blocks that are assembled into the macromolecules; these include amino acids, nucleotides, lipid components, peptidoglycan monomers, and polyamines (Neidhardt et al., 1990). All the building blocks are derived from a central pool of a dozen core metabolites comprising glucose-6-phosphate, fructose-6-phosphate, ribose-5-phosphate, erythrose-5-phosphate, triose-phosphate, 3-phosphoglycerate, phosphoenolpyruvate, pyruvate, acetyl-CoA, α-ketoglutarate, succinyl CoA, and oxaloacetate (Neidhardt et al., 1990). The combined cost of synthesis for all required monomers from these twelve metabolites to generate one gram-cell d/w equals 0.018 mol ATP, -0.0035 mol NADH, and 0.017 mol NADPH (Neidhardt et al., 1990). Generation of NAD(P)H from NAD(P)$^+$ requires 1.5 ATP molecules (Sweetman and Griffiths, 1971; Noguchi et al., 2004). Thus, the glucose equivalent of the energetic requirement of 1 g d/w cell is as follows:

$(0.018$ mol ATP $- 0.0035$ mol NADH $\times 1.5$ ATP per NADH+
0.017 mol NADPH $\times 1.5$ ATP per NADPH$) \times$
$(0.034$ molecules of glucose per ATP$) \times 180$ g/mol $= 0.23$ g glucose per gram-cell .

Similar calculations yield that energetic requirements for glucose are 0.13 g/(gram-cell) to synthesise the precursors for protein production, 0.034 g/(gram-cell) to synthesise precursors for RNA production, and 0.0009 g/(gram-cell) to synthesise precursors for glycogen production.

Glucose investment in macro-chemical components. Synthetic machinery (M_0) contains both RNA and proteins. Accordingly, we estimate the total amount of the glucose required for these purposes in the following way:

$$
\begin{aligned}
&\beta_0 \times (0.18 \text{ g glucose as a building block for RNA production} \\
&+ \ 0.036 \text{ g glucose to fuel RNA production}) \\
&+ \ 0.196 \times (0.73 \text{ g glucose as a building block for protein production} \\
&+ \ 0.26 \text{ g glucose as to fuel protein production}) \\
&= \ 0.33 \text{ g glucose per gram-cell for synthetic machinery .}
\end{aligned}
$$

A similar calculation for growth machinery (M_G) yields:

$$
\begin{aligned}
&(1 - \beta_0) \times (0.18 \text{ g glucose as a building block for RNA production} \\
&+ \ 0.036 \text{ g glucose to fuel RNA production}) \\
&+ \ 0.338 \times (0.73 \text{ g glucose as a building block for protein production} \\
&+ \ 0.26 \text{ g glucose to fuel protein production}) \\
&= \ 0.42 \text{ g glucose per gram-cell for growth machinery .}
\end{aligned}
$$

A similar calculation for assimilatory machinery ($\sum_{i=1}^{n} M_i$) yields:

$$
\begin{aligned}
&0.072 \times (0.73 \text{ g glucose as a building block for protein production} \\
&+ \ 0.26 \text{ g glucose to fuel protein production}) \\
&= \ 0.071 \text{ g glucose per gram-cell for uptake machinery .}
\end{aligned}
$$

To estimate the amount of glucose invested in the structural component, we subtract, from the total glucose requirement for 1 gram-cell, the requirements for the catalytic machinery components as well as the glycogen reserves as found in a cell grown under standard conditions. This gives:

$$
\begin{aligned}
&(1.25 \text{ g glucose as a building block for production of 1 gram-cell} \\
&+ \ 0.37 \text{ g glucose to fuel production of 1 gram-cell}) \\
&- \ 0.33 \text{ g glucose for } M_0 \\
&- \ 0.42 \text{ g glucose for } M_G \\
&- \ 0.071 \text{ g glucose for } (M_1 + \cdots + M_n) \\
&- \ 0.0289 \text{ g glucose fueling synthesis of glycogen reserves} \\
&= \ 0.77 \text{ g glucose per gram-cell to produce the structural component .}
\end{aligned}
$$

Rate of glucose reserve consumption. By the scaling relations outlined in Section 2 we have

$$\sigma_{ji} = \frac{\widetilde{\sigma}_{ji}\widetilde{\phi}_i}{\widetilde{\sigma}_{jW}\widetilde{\phi}_0}\hat{m} \, .$$

Since we assume that $\sigma_{ji} = \sigma_j$ for $i \in \{0, 1, \ldots, n, G\}$, for $i = 0$ we have:

$$\sigma_j = \frac{\widetilde{\sigma}_{j0}\widetilde{\phi}_0}{\widetilde{\sigma}_{jW}\widetilde{\phi}_0}\hat{m} = \frac{\widetilde{\sigma}_{j0}}{\widetilde{\sigma}_{jW}}\hat{m} \, ,$$

and we therefore calculate the stoichiometric coefficient σ_{Gl} as follows:

$$\sigma_{Gl} = \frac{\widetilde{\sigma}_{Gl,0}}{\widetilde{\sigma}_{Gl,W}}\hat{m} \, , \tag{A.2}$$

where $\hat{m} = M_0/W$. The coefficients $\widetilde{\sigma}_{Gl,0}$ and $\widetilde{\sigma}_{Gl,W}$ in eqn (A.2) denote the amounts of glucose required to produce a unit of, respectively, synthetic machinery or structural component. Accordingly, we have

$$\widetilde{\sigma}_{Gl,0} = \frac{0.33 \text{ g glucose per gram-cell for } M_0 \text{ production}}{0.232 \text{ g of } M_0 \text{ per gram-cell}} = 1.4 \text{ g glucose per g } M_0 \, ,$$

$$\widetilde{\sigma}_{Gl,W} = \frac{0.77 \text{ g glucose per gram-cell for } W \text{ production}}{0.436 \text{ g of } W \text{ per gram-cell}} = 1.8 \text{ g glucose per g of } W \, ,$$

and using $\hat{m} = M_0/W = 0.53$ g of M_0 per g of W, we find

$$\sigma_{Gl} = \frac{1.4 \text{ g glucose per g } M_0 \times 0.53}{1.8 \text{ g glucose per g } W} = 0.4 \, .$$

Appendix A.4. Stoichiometric coefficients related to nitrogen

Nitrogen requirements. A single gram dry weight of cellular mass contains 0.097 g nitrogen dispersed over its proteinaceous contents, and 0.035 g nitrogen contained in its RNA (Neidhardt et al., 1990). Accordingly, nitrogen requirements for the production of each type of machinery

are as follows:

$$\beta_0 \times 0.035 \text{ g nitrogen per gram-cell for RNA}+$$
$$0.196 \times 0.097 \text{ g nitrogen per gram-cell for protein} =$$
$$0.04 \text{ g nitrogen per gram-cell for synthetic machinery production};$$
$$(1 - \beta_0) \times 0.035 \text{ g nitrogen per gram-cell for RNA}+$$
$$0.338 \times 0.097 \text{ g nitrogen per gram-cell for protein} =$$
$$0.047 \text{ g nitrogen per gram-cell for growth machinery production};$$
$$0.072 \times 0.097 \text{ g nitrogen per gram-cell for protein} =$$
$$0.007 \text{ g nitrogen per gram-cell for assimilatory machinery production}.$$

According to Yuan et al. (2006), glutamate ($C_5H_9NO_4$, 147 g/mol, the main nitrogen reserve in *E. coli*) comprises 100.55×10^{-6} mol per gram-cell. In terms of stoichiometric reckoning, only the nitrogen atoms in these glutamate molecules are assigned to the reserve, whereas the glutamine body is assigned to the structural component, in accordance with the biochemical notion of transaminase reactions to store the cell's temporary nitrogen surplus onto these bodies (Neidhardt et al., 1990). We have

$$100.55 \times 10^{-6} \text{ mol per gram-cell} \times 14 \text{ g/mol} =$$
$$0.0014 \text{ g nitrogen per gram-cell attributed to nitrogen reserve}.$$

An *E. coli* cell contains 14% nitrogen d/w (Neidhardt et al., 1990) and thus

$$0.14 - (0.04 + 0.047 + 0.007 + 0.0014) =$$
$$0.045 \text{ g nitrogen per gram-cell in the structural component}.$$

Rate of nitrogen reserve consumption. To estimate the stoichiometric coefficient σ_N we use the following scaling equation:

$$\sigma_N = \frac{\widetilde{\sigma}_{N,0}}{\widetilde{\sigma}_{N,W}} \hat{m}, \tag{A.3}$$

where $\hat{m} = M_0/W$. The coefficients $\widetilde{\sigma}_{N,0}$ and $\widetilde{\sigma}_{N,W}$ denote the nitrogen amount needed to produce a unit of synthetic machinery or structural component, respectively. Accordingly,

$$\widetilde{\sigma}_{N,0} = \frac{0.04 \text{ g N per gram-cell for } M_0 \text{ production}}{0.232 \text{ g of } M_0 \text{ per gram-cell}} = 0.17 \text{ g N per g } M_0,$$
$$\widetilde{\sigma}_{N,W} = \frac{0.045 \text{ g N per gram-cell for } W \text{ production}}{0.436 \text{ g of } W \text{ per gram-cell}} = 0.1 \text{ g N per g } W,$$

and using $\hat{m} = M_0/W = 0.53$ g of M_0 per g of W, we find

$$\sigma_N = \frac{0.17 \text{ g N per g } M_0 \times 0.53}{0.1 \text{ g N per g } W} = 0.8.$$

Nitrogen cell quota. By definition, the nitrogen cell quota is its intracellular density (amount per cell, which can roughly by thought of as an average concentration; Droop, 1968). In terms of the state scaled variables of the macro-chemical model we have the following linear stoichiometric equation (assuming $n = 1$):

$$Q_N = \kappa_{m,0}m_0 + \kappa_{m,G}m_G + \kappa_{m,N}m_N + \kappa_{x,N}x_N + \kappa_W , \tag{A.4}$$

where κ_* is the amount of nitrogen attributed to the corresponding component $*$ in gram per cell. Following this definition of κ_*, we express $\kappa_{x,N}x_N$ as follows

$$\kappa_{x,N}x_N = \frac{X_N}{\gamma_W W} ,$$

where γ_W is the number of cells that corresponds to one gram of structural component W. Therefore together with scaling from eqn (4) we have

$$\kappa_{x,N}x_N = \frac{W\widetilde{\sigma}_{N,W}x_N}{\gamma_W W} = \frac{\widetilde{\sigma}_{N,W}x_N}{\gamma_W} ,$$

whence

$$\kappa_{x,N} = \frac{\widetilde{\sigma}_{N,W}}{\gamma_W} = 1.25 \times 10^{-14} \text{ g N per cell attributed to the nitrogen reserve .}$$

Reasoning similarly, we represent $\kappa_{m,i}m_i$ for $i \in \{0, N, G\}$ in the following form:

$$\kappa_{m,i}m_i = \frac{\text{g N}}{\text{g } M_i} \times \frac{\text{g } M_i}{\text{cell}} = \frac{\text{g N}}{\text{g } M_i} \times \frac{\text{g } M_i}{\text{g } W} \times \frac{\text{g } W}{\text{cell}} = \frac{\text{g N}}{\text{g } M_i} \times \frac{m_i\widehat{m}\widetilde{\phi}_i}{\widetilde{\phi}_0} \times \frac{\text{g } W}{\text{cell}} ,$$

whence

$$\kappa_{m,i} = \frac{\text{g N}}{\text{g } M_i} \times \frac{\widehat{m}\widetilde{\phi}_i}{\widetilde{\phi}_0} \times \frac{\text{g } W}{\text{cell}} .$$

Using this expression, we obtain the following values for the weighting coefficients:

$$\kappa_{m,0} = 1.13 \times 10^{-14} \text{ g N per cell attributed to the synthetic machinery ,}$$

$$\kappa_{m,G} = 4.39 \times 10^{-15} \text{ g N per cell attributed to the growth machinery ,}$$

$$\kappa_{m,N} = 2.38 \times 10^{-13} \text{ g N per cell attributed to the nitrogen assimilatory machinery .}$$

The last coefficient κ_W can be expressed as follows:

$$\kappa_W = \frac{\text{g N}}{\text{g } W} \times \frac{\text{g } W}{\text{cell}} = 1.25 \times 10^{-14} \text{ g N per cell attributed to the structural component .}$$

In these units, eqn (A.4) takes on the following form:

$$Q_N = 1.13 \times 10^{-14}m_0 + 4.39 \times 10^{-15}m_G + 2.38 \times 10^{-13}m_N + 1.25 \times 10^{-14}x_N + 1.25 \times 10^{-14} =$$
$$1.13 \times 10^{-14}m_0 + 4.39 \times 10^{-15}\widetilde{\mu}(\widetilde{\phi}_0\psi_W)^{-1} + 2.38 \times 10^{-13}m_N + 1.25 \times 10^{-14}x_N + 1.25 \times 10^{-14} , \tag{A.5}$$

since it follows from the scaling (Section 2) and the definition of the specific growth rate that $\widetilde{\mu} = \mu\widetilde{\phi}_0 = m_G\psi_W\widetilde{\phi}_0$.

Appendix A.5. Stoichiometric coefficients related to phosphorus

Phosphorus requirements for the cell components production. According to Nesmeyanova (2000), polyphosphate, which constitutes the main phosphorus reserve, accounts on average for ~ 0.003 g per gram-cell d/w. Since PO_3H units weighs 80 g/mol and phosphorus weighs 31 g/mol, we should assign $0.003 \times 31/80 = 0.001$ g of P per gram-cell to the phosphorus reserve.

Assuming that the four bases guanine, adenine, cytosine, and uracil are equally abundant (Riley et al., 2006), we find that an RNA unit weighs $80 + 115 + (150 + 134 + 110 + 111)/4 = 321.25$ g/mol, which implies that RNA requires $31/321.25 = 0.096$ g P per gram-cell. Accordingly, phosphorus requirements for the production of synthetic and growth machineries are as follows:

$$\beta_0 \times 0.096 \text{ g P per g of RNA} \times 0.2053 \text{ g of RNA per gram-cell} =$$
$$0.012 \text{ g P per gram-cell for synthetic machinery} .$$
$$(1 - \beta_0) \times 0.096 \text{ g P per g of RNA} \times 0.2053 \text{ g RNA per gram-cell} =$$
$$0.008 \text{ g P per gram-cell for growth machinery} .$$

An average *E. coli* cell is about 3% phosphorus d/w (Neidhardt et al., 1990), whence we conclude that

$$0.03 \text{ g P per gram-cell} - (0.012 \text{ g P per gram-cell in the synthetic machinery}$$
$$+ \quad 0.008 \text{ g P per gram-cell in the growth machinery}$$
$$+ \quad 0.001 \text{ g P per gram-cell in the reserve})$$
$$= \quad 0.009 \text{ g P per gram-cell in the structural component} .$$

Rate of phosphorus reserve consumption. We estimate the stoichiometric coefficient σ_P in accordance with the following scaling equation:

$$\sigma_P = \frac{\widetilde{\sigma}_{P,0}}{\widetilde{\sigma}_{P,W}} \hat{m} \tag{A.6}$$

with $\hat{m} = M_0/W$. The coefficients $\widetilde{\sigma}_{P,W}$ and $\widetilde{\sigma}_{P,0}$ express, respectively, how much phosphorus is required to synthesise one unit of the structural component and of the synthetic machinery. Thus we obtain:

$$\widetilde{\sigma}_{P,0} = \frac{0.012 \text{ g of P per gram-cell for } M_0 \text{ production}}{0.232 \text{ g of } M_0 \text{ per gram-cell}} = 0.052 \text{ g of P per g of } M_0 ,$$

$$\widetilde{\sigma}_{P,W} = \frac{0.009 \text{ g of P per gram-cell for } W \text{ production}}{0.436 \text{ g of } W \text{ per gram-cell}} = 0.02 \text{ g of P per g of } W .$$

Therefore we have:

$$\sigma_P = \frac{0.052 \text{ g of P per g of } M_0 \times 0.53 \text{ g of } M_0 \text{ per g of } W}{0.02 \text{ g of P per g of } W} = 1.4 .$$

Appendix A.6. Maintenance

To estimate the maintenance coefficients c_j we use the scaling equation (Section 2):

$$c_j = \frac{\widetilde{c}_j}{\widetilde{\sigma}_{jW}\widetilde{\phi}_0} \ , \tag{A.7}$$

where the coefficient $\widetilde{c}_j$ expresses the amount of substrate j per unit of structural component per unit of time required by the cell to maintain essential processes and structures that are not related to its growth. This parameter can be estimated by means of the following definition of the maintenance coefficient (Pirt, 1965):

$$m = a/Y \ , \tag{A.8}$$

where a denotes the specific maintenance rate, a typical value for *E. coli* being ~ 0.03 h $^{-1}$ (Neidhardt et al., 1990). The parameter Y is the yield coefficient for a substrate used for growth, which is estimated as 0.25 g of cell dry weight per g glucose for *E. coli* growing on glucose (Henry, 1969). Therefore we can calculate the maintenance coefficient $\widetilde{c}_{Gl}$ for *E. coli* growing on glucose as follows:

$$\widetilde{c}_{Gl} = \frac{0.03/3600 \text{ per second}}{0.25 \text{ gram-cell per g glucose} \times 0.436 \text{ g } W \text{ per gram-cell}}$$
$$= 7.6 \times 10^{-5} \text{ g glucose per g } W \text{ per second} \ ,$$

whence the scaled coefficient takes on the following form:

$$c_{Gl} = \frac{7.6 \times 10^{-5} \text{ g glucose per g } W \text{ per second}}{1.8 \text{ g glucose per g } W \times 0.0053 \text{ per second}} = 0.008 \ .$$

Appendix A.7. Adjustments for eukaryotes

Inasmuch as *E. coli* is much more extensively documented than almost any other microorganism, it is tempting to treat the *E. coli*-based estimates as quasi-universal. This can be expected to be warranted to some extent, the more so as the parameters express intrinsic, biochemically universal properties. For instance, the storage compounds that are accumulated in the cells can probably be regarded as comparable, as many algal species accumulate glycogen (West, 1916), amino acids (Dortch et al., 1984), and polyphosphate (Rhee, 1973). Nonetheless, eukaryotic unicellular organisms are quite distinct from the prokaryote *E. coli*, and therefore this porting of stoichiometric estimates must be considered with some care, and adjusted wherever data are available for the eukaryotic species analysed in the main text. Since the cell quota is calculated on a per cell basis rather than g d/w, the weighting coefficients (κ-type parameters) need to be revised, using the reported dry weight of 2.9×10^{-10} g/cell for *Skeletonema costatum* (Pan et al., 2010).

Adjustments for nitrogen cell quota for Skeletonema costatum. The weighing coefficients for the nitrogen cell quota equation are adjusted as follows:

$$\kappa_{x,N} = 1.3 \times 10^{-11} \text{ g N per cell attributed to the nitrogen reserve },$$

$$\kappa_{m,0} = 1.2 \times 10^{-11} \text{ g N per cell attributed to the synthetic machinery },$$

$$\kappa_{m,G} = 4.5 \times 10^{-12} \text{ g N per cell attributed to the growth machinery },$$

$$\kappa_{m,N} = 2.45 \times 10^{-10} \text{ g N per cell attributed to the nitrogen assimilatory machinery },$$

$$\kappa_{W} = 1.3 \times 10^{-11} \text{ g N per cell attributed to the structural component }.$$

Table A.2: Assignment of *E. coli* proteins to macro-chemical components

ine Synthetic M_0 ine	Uptake $M_1, \ldots, M_n$	Growth M_G	Structural W
Ribosome-associated	Path to core metabolism	Agmatine biosynthesis	Catabolism
Rlml	AnsA	SpeA	AsnB
RlmN	AspA	SpeB	ClpP
RluB	CysQ	Amino-acid biosynthesis	DacA
RluD	DadA	ArgA	DacC
RmsA	GadA	ArgB	Dcp
Rnc	GcvP	ArgC	DegQ
RsgA	LtaE	ArgD	Ggt
RsmB	ManA	ArgE	GlmS
RsmC	MtlD	ArgG	GuaA
RsuA	TreA	ArgH	HslV
SrmB	Nutrient uptake	ArgI	LdcA
Yfif	AlsB	AroA	LexA
TypA	AraF	AroB	Lon
RimM	ArgT	AroC	Map
RaiA	ArtI	AroG	OmpT
RbfA	ArtJ	AroK	PepA
YchF	ArtP	Asd	PepB
YbcJ	ChbB	AspC	PepD
YibL	Crr	CysE	PepE
RoxA	CysA	CysK	PepN
YjgA	CysP	CysM	PepP
Der	Dppa	DapB	PepQ
RimP	DppD	DapD	PepT
YihI	DppF	DapE	PmbA
YjeE	FepB	DapF	Prc
HflX	FruA	DkgA	PrlC
RsmI	FruB	HisB	PurF
Era	GalE	HisC	SohB
RlmM	GatA	HisD	TldD
Ribosomal	GlnH	HisF	YajL
RplA	GlnQ	HisG	YegQ
RplB	GltI	HisH	YggG
RplC	GsiB	HisI	YhbO

Table A.2: Assignment of *E. coli* proteins to macro-chemical components

ine Synthetic M_0 ine	Uptake $M_1, \ldots, M_n$	Growth M_G	Structural W
RplD	HisJ	IlvB	Chaperones/folding
RplE	HisP	IlvC	CbpA
RplF	KgtP	IlvD	ClpA
RplI	LivF	IlvE	ClpB
RplJ	LivG	IlvH	ClpX
RplK	LivJ	IlvI	CspC
RplL	LivK	LeuA	CspD
RplM	LolD	LeuC	CspE
RplN	LptB	LeuD	DegP
RplO	LptF	LysA	DnaJ
RplP	LptG	LysC	DnaK
RplQ	LsrB	MetA	DsbA
RplR	MalE	MetB	DsbC
RplS	MalK	MetC	DsbG
RplT	ManX	MetE	FklB
RplU	ManY	MetK	FkpA
RplV	ManZ	MetL	FkpB
RplW	MetN	Mtn	FtsH
RplX	MetQ	PheA	GroL
RplY	MglA	ProA	GroS
RpmA	MlaD	ProB	GrpE
RpmB	MlaF	ProC	GrxB
RpmC	ModA	RidA	GrxC
RpmD	ModF	SerA	GrxD
RpmE	MppA	SerC	HdeB
RpmF	MsbA	ThrA	HscA
RpmG	MtlA	ThrB	HscB
RpmH	NagE	ThrC	HslO
RpsA	NlpA	TrpA	HslU
RpsB	OmpA	TrpB	HtpG
RpsC	OmpC	TrpC	NfuA
RpsD	OmpF	TrpD	PpiA
RpsE	OppA	TrpE	PpiB
RpsF	OsmF	TyrA	PpiC
RpsG	PhoP	TyrB	PpiD
RpsH	PotA	Usg	SecB
RpsI	PotD	Cell division	Skp
RpsJ	PotF	Fic	SlyD
RpsK	PstS	FtsA	SurA
RpsL	PtsG	FtsE	Tig
RpsM	PtsH	FtsZ	TrxA
RpsN	PtsI	MinC	TrxC
RpsO	PtsN	MinD	YbbN
RpsP	PtsP	MinE	ProQ
RpsQ	RbsD	MreB	YcdY
RpsR	SapA	MukE	BepA
RpsS	SufC	RodZ	Chemotaxis

33

Table A.2: Assignment of *E. coli* proteins to macro-chemical components

ine Synthetic M_0	Uptake $M_1, \ldots, M_n$	Growth M_G	Structural W
ine			
RpsT	ThiB	Slt	FliY
RpsU	UgpB	ZapA	RbsB
Sra	YadG	ZapB	Defense
YqjD	YdcS	ZipA	Ahpc
Hpf	YecC	ObgE	ArcA
RNA-related	YgiS	EngB	ArcB
AlaS	YtfQ	FtsP	Bcp
ArgS	MscS	DamX	DcyD
AsnS	TolB	ZapD	Dps
AspS	MlaC	MatP	FrdA
CysS	DcrB	NlpI	FrdB
Fmt	EfeO	RlpA	GlnB
GlnS	AroP	Cell envelope synthesis	KatE
GltX	TolQ	AccA	KatG
GlyQ	CorC	AccB	LuxS
GlyS	Tsx	AccC	NarL
HisS	PhoU	AccD	NarP
IleS	GadC	AcpP	OtsA
LeuS	CorA	AnmK	SodA
LysS	ChaB	BtuE	SodB
LysU	SstT	Cld	SodC
MetG	TrkA	DhaK	SolA
MnmA	LamB	DhaL	SpeG
PheS	FadL	FabA	Tpx
PheT		FabB	WrbA
ProS		FabD	Yfid
RpoA		FabF	Yqhd
RpoB		FabG	Metabolic intermediates
RpoC		FabH	AceA
RpoD		FabI	AceB
RpoE		FabZ	AceE
RpoN		FadA	AceF
RpoS		FadB	AckA
RpoZ		FadE	AcnA
SerS		FadI	AcnB
ThrS		FadJ	Acs
TrpS		FadM	AdhE
TyrS		Ffh	Agp
ValS		FtsY	ArnC
YihD		GalF	AtpA
YhbY		Glf	AtpC
YgfZ		GlpK	AtpD
RraA		GpsA	AtpF
LepA		KdsA	AtpG
YceD		KdsB	AtpH
YciO		KdsC	BglA
CmoA		LpcA	CobB

34

Table A.2: Assignment of *E. coli* proteins to macro-chemical components

ine Synthetic M_0	Uptake $M_1,\ldots,M_n$	Growth M_G	Structural W
ine			
RseB		LpxA	CydA
RimN		LpxB	CydB
MnmE		LpxD	CyoA
RapZ		Mpl	CyoB
Transcription		MrcB	DeoC
AllR		MurA	Dld
ArgP		MurC	Eda
Crl		MurD	Eno
Crp		MurE	FbaA
CysB		MurF	FbaB
DksA		PlsB	Fbp
FadR		Psd	FolA
Fnr		PssA	FolD
FruR		RfaD	FrmA
Fur		RfaE	FucO
GlpR		TesA	FumA
GntR		TesB	GabD
HupA		UgpQ	GabT
HupB		YidC	GalM
IscR		YbiS	GapA
Lrp		MdoG	GarR
MalT		LolA	Gcd
MetJ		LptA	GcvH
MhpR		BamC	GcvT
MprA		CpoB	GhrA
NadR		BamB	GhrB
NagC		BamD	GlcB
NikR		BamA	Glk
NrdR		YnhG	GlmM
OsmE		LpoB	GlmU
OxyR		MipA	GloA
PdhR		WbbI	GloB
PurR		LpoA	GltA
SlyA		LolB	GlyA
TrpR		MdoD	Gnd
TyrR		YcjG	Gor
YqgE		ErfK	GpmA
Zur		LptD	GpmM
NusG		LapB	Gst
BolA		Cofactor biosynthesis	HchA
YebC		BioD	Icd
Cra		CoaA	KdgK
KdgR		Dxs	LdhA
YehT		FolE	LldD
YciT		Fre	Lpd
YhgF		FtnA	MaeA
RapA		HemB	MaeB

35

Table A.2: Assignment of *E. coli* proteins to macro-chemical components

ine Synthetic M_0	Uptake $M_1, \ldots, M_n$	Growth M_G	Structural W
ine			
Translation		HemD	Mdh
Efp		HemE	MetF
Frr		HemG	MetH
FusA		HemX	MgsA
InfA		Iscs	MurQ
InfB		IspA	NagB
InfC		IspB	NagZ
PrfC		IspG	Ndh
Tsf		IspH	NuoA
TufA		LipA	NuoB
YeiP		MenB	NuoC
EttA		MoaC	NuoF
YbaK		MoaD	NuoG
SelB		MoaE	NuoI
		NadA	Pck
		NadC	PfkA
		NadE	PfkB
		NadK	PflB
		PanB	Pgi
		PanC	Pgk
		PdxB	Pgl
		PdxH	Pgm
		PdxJ	PoxB
		PncA	Ppa
		PncB	Ppc
		PntA	PpsA
		PntB	Prs
		QueC	Pta
		RfbA	PurH
		RfbB	PurN
		RfbC	PurT
		RfbD	PykA
		RibB	PykF
		RibC	RbsK
		RibD	Rpe
		RibE	RpiA
		SthA	SdhA
		SufS	SdhB
		ThiC	SdhD
		ThiD	SseA
		ThiE	SucA
		ThiF	SucB
		ThiG	SucC
		ThiL	SucD
		ThiM	TalA
		UbiB	TalB
		UbiD	ThyA

36

Table A.2: Assignment of *E. coli* proteins to macro-chemical components

ine Synthetic M_0 ine	Uptake $M_1, \ldots, M_n$	Growth M_G	Structural W
		UbiE	TktA
		UbiF	TktB
		UbiG	TpiA
		MoaB	YccX
		MoeA	YdbK
		UbiJ	YeaD
		DNA replication	YtjC
		DnaA	Zwf
		DnaN	IscU
		DnaX	YeeX
		GyrA	HinT
		GyrB	YdgH
		IhfA	YdhR
		IhfB	YgiN
		LigA	ErpA
		PolA	Ivy
		Purine metabolism	GstB
		Pyrimidine metabolism	Fdx
		Rob	ElbB
		SeqA	YdjN
		Ssb	SgcQ
		TopA	AzoR
		YbaB	MioC
		GreA	NagD
		YdaM	MenI
		Fatty acid biosynthesis	RcnB
		Cfa	IscA
		GnsB	Dtd
		Glutamate biosynthesis	FdhE
		GdhA	UcpA
		Glutamine biosynthesis	YgiF
		GlnA	EutL
		GltB	YcbX
		GltD	FrsA
		Glutathione biosynthesis	CsdE
		GshB	MpaA
		Protein biosynthesis	CpdA
		Def	PaaY
		FolX	GutQ
		PncC	Pka
		Protoporphyrin biosynthesis	Repair
		HemL	Dut
		HemY	HelD
		Selenophosphate biosynthesis	Mfd
		SelD	MsrA
		Spermidine biosynthesis	MsrB
		SpeE	Mug

Table A.2: Assignment of *E. coli* proteins to macro-chemical components

ine Synthetic M_0 ine	Uptake $M_1, \ldots, M_n$	Growth M_G	Structural W
		Sulfide biosynthesis	MutL
		CysH	NrdA
		CysI	NrdB
		CysJ	RdgC
			RecA
			UvrA
			UvrB
			UvrD
			XseB
			XthA
			RNA degradation
			Pnp
			Ppk
			RhlB
			Rho
			Rnb
			Rne
			Rnr
			RraB
			Ydfg
			Orn
			RNA modification
			Tgt
			TrmJ
			Secretion
			AcrA
			CopA
			CusB
			CusC
			CusF
			SecA
			SecD
			SecG
			SecY
			TolC
			YajC
			YebF
			MsyB
			AcrB
			Storage-related
			CsrA
			GlgA
			GlgB
			GlgC
			GlgP
			MalP
			Bfr

Table A.2: Assignment of *E. coli* proteins to macro-chemical components

ine Synthetic M_0 ine	Uptake $M_1,\ldots,M_n$	Growth M_G	Structural W
			Transcriptional repressors
			BaeR
			BasR
			CpxR
			Hns
			OmpR
			RcsB
			RcsD
			RstA
			StpA
			SuhB
			UvrY
			NusA
			NusB
			Rof
			Rsd
			RcnR
			YjdC
			FrmR
			MtfA
			ExuR
			FabR
			LrhA
			Defence
			UspA
			OsmY
			YajQ
			OsmC
			YifE
			HdeA
			SspA
			YggX
			UspG
			YfbU
			YggE
			ElaB
			PspA
			IbaG
			ChrR
			UspE
			AhpF
			UspF
			Tas
			YbgI
			CueO
			Slp
			SspB

Table A.2: Assignment of *E. coli* proteins to macro-chemical components

ine Synthetic M_0 ine	Uptake $M_1, \ldots, M_n$	Growth M_G	Structural W
			YiiM
			MscL
			SlyX
			UspD
			SbmC
			TehB
			YmdB
			YfcF
			CstA
			MobA
			PspB
			Blc
			Cell envelope
			Lpp
			YbaY
			YhcB
			Pal
			Redox reactions
			MsrC
			CyaY
			MdaB
			FldA
			YgjR
			YdgJ
			QorB

Based on data reported by Valgepea et al. (2013) using the *proteomaps* data visualisation tool by Liebermeister et al. (2014) .